Characterizing the Flammability of Storage Commodities Using an Experimentally Determined B-number

by

Kristopher Overholt

A Thesis

Submitted to the Faculty

of the

WORCESTER POLYTECHNIC INSTITUTE

in partial fulfillment of the requirements for the

Degree of Master of Science

in

Fire Protection Engineering

December 2009

by

_____

Kristopher James Overholt

Approved:

_____

Professor Ali Rangwala, Advisor

_____

Professor Kathy Notarianni, Head of Department

_____

Jonathan Perricone, Consultant, Creative FPE Solutions, Inc.

Abstract

In warehouse storage applications, it is important to classify the burning behavior of commodities and rank them according to material flammability for early fire detection and suppression operations. In this study, the large-scale effects of warehouse fires are decoupled into separate processes of heat and mass transfer. As a first step, two nondimensional parameters are shown to govern the physical phenomena at the large-scale, a mass transfer number, and the soot yield of the fuel which controls the radiation observed in the large-scale. In this study, a methodology is developed to obtain a mass-transfer parameter using mass-loss (burning rate) measurements from bench-scale tests. Two fuels are considered, corrugated cardboard and polystyrene. Corrugated cardboard provides a source of flaming combustion in a warehouse and is usually the first item to ignite and sustain flame spread. Polystyrene is typically used as the most hazardous product in large-scale fire testing. A mixed fuel sample (corrugated cardboard backed by polystyrene) was also tested to assess the feasibility of ranking mixed commodities using the bench-scale test method. The nondimensional mass transfer number was then used to model upward flame propagation on 20-30 foot stacks of Class III commodity consisting of paper cups packed in corrugated cardboard boxes on rack-storage. Good agreement was observed between the model and large-scale experiments during the initial stages of fire growth.

Keywords:

upward flame spread, flame height, commodity classification, B number, warehouse fire, scale modeling

Acknowledgements

Special thanks to Randall Harris at the WPI Fire Science Laboratory for assistance with the cone calorimeter tests. Commodity samples were generously donated by David LeBlanc at Tyco International. Corrugated Corrugated cardboard samples were generously donated by Sam Abbott at Abbot-Action in Canton, MA.

Special thanks to Dr. Kathy Notarianni, for her generous support, motivation, and making it possible for my experience at WPI to become an exciting reality.

A big thanks to my advisor, Prof. Ali Rangwala, for spending the time to learn my strengths and weaknesses, and pushing me to my intellectual limits. His motivation for teaching others, enthusiasm for thinking along unconventional means, and intellectual merit were always a pleasure to work with.

Finally, I'd like to thank my fiancée, Katie, for her unconditional support and loving encouragement during the strenuous times of graduate research; my parents, Rick and Noemi, for always inspiring me to do the absolute best that I can in this world; and God, for providing me with the strength and continued means to expand my knowledge and share it with others.

Contents

List of Tables

List of Figures

Nomenclature

Symbols

A_l	Eq. 11a
A_t	Eq. 11b
B	Mass transfer number, Spalding number $(-)$
c_p	Specific heat $(J/g \cdot K)$
D	Species diffusivity (m^2/s)
d	Panel separation distance (m)
Gr	Grashof number $(-)$
ΔH_c	Heat of combustion (J/g)
ΔH_g	Heat of gasification (J/g)
g	Acceleration due to gravity (m/s^2)
h	Heat transfer coefficient (W/m^2K)
h_c	Convective heat transfer coefficient (W/m^2K)
h_r	Radiant heat transfer coefficient (W/m^2K)
k	Thermal conductivity $(W/m \cdot K)$
$\dot{m}''$	Mass-loss rate $(g/m^2 \cdot s)$
Nu	Nusselt number $(-)$
Pr	Prandtl number $(-)$
Q	Energy losses at fuel surface (W)
$\dot{q}''_A$	Volumetric heat release rate (kW/m^3)
$\dot{q}''_c$	Convective heat flux per unit area (kW/m^2)
$\dot{q}''_{loss}$	Surface heat loss rate (kW/m^2)
$\dot{q}''_r$	Radiant heat flux per unit area (kW/m^2)
$\dot{q}''(x)$	Surface heat flux per unit area (kW/m^2)
$\dot{q}''(0)$	Surface heat flux at height x_p (kW/m^2)

$\dot{q}'_F$	Rate of forward heat transfer per unit width (W/m)
$\dot{q}'_c$	Rate of heat release by combustion per unit width (W/m)
r	Mass consumption number $(Y_{O,\infty}/\nu_s)$
T_m	Average temperature between flame and fuel surface (K)
T_p	Fuel pyrolysis temperature (K)
T_∞	Ambient temperature (K)
v_s	Stoichiometric oxygen-mass fuel ratio $(-)$
U	Free stream velocity (K)
V_{xp}	Velocity of pyrolysis front (m/s)
w	Panel/sample width (m)
x_f	Flame height (m)
x_p	Pyrolysis height (m)
Y_{O_2}	Mass fraction of oxygen (g/g)
Y_g	Soot yield of combustion gases (g/g)
Y_s	Soot yield of fuel (g/g)

Greek Symbols

α	Thermal diffusivity (m^2/s)
β	Thermal expansion coefficient $(1/K)$
χ	Fraction of flame radiation lost to the environment $(-)$
δ	Preheat distance (m)
ϵ	Emissivity $(-)$
ρ	Density (g/m^3)
μ	Viscosity $(kg/m \cdot s)$
ν	Kinematic viscosity (m^2/s)
Φ	Forward heating parameter $(\dot{q}'_F/\dot{q}_c)$
σ	Stefan-Boltzmann Constant (W/m^2K^4)

τ	Shear stress at surface (Pa)
ς_f	Nondimensional flame height $(-)$
ς_p	Nondimensional panel height $(-)$

Subscripts

F	Fuel
f	Flame
g	Gas
m	Mean
s	Solid
∞	Ambient

1 Introduction

A recent devastating fire loss in 2007 at Tupperware Brand Corp.'s manufacturing and distribution center in Hemingway, South Carolina (S.C.), US, was potentially due to shortcomings in the current approach to commodity classification, which is a baseline for designing automatic sprinkler system protection. The warehouse in S.C. was protected throughout by an automatic sprinkler system installed in accordance with NFPA 13 requirements, yet the end result was a total loss [1]. Significant blame has been placed on the fire department for shutting down the sprinkler system in favor of manual suppression after 17 hours of burning. Such a duration is not indicative of an event that was under control by the automatic system. If the system performed as intended, the experimental data on which the design was presumably based should be used as a starting point for discussion.

The storage of various commodities in large warehouses poses a unique hazard to occupants, firefighters, and surrounding communities due to the concentration of flammable, often toxic materials stored to heights of up to 16 meters (50 ft). A recent fire at Tupperware Brands Corp.'s manufacturing and distribution center in Hemingway, South Carolina has brought increased attention to the current need for improvement of large warehouse fire protection [1]. The fire was ignited by an electrical spark in a rack and quickly spread, completely destroying the 15,329 m^2 facility over a period of 35 hours. The warehouse was fully protected by in-rack sprinklers, installed to current codes and standards, yet the protection system still failed. A series of similar losses have occurred, as summarized in Table 1 [2]. The impact of warehouse fires ranges from economical losses to firefighter safety to the environmental impact of runoff water from firefighting operations.

Current methods for commodity classification are outlined by FM Global Data Sheet 8-1 and the National Fire Protection Association (NFPA) building and fire codes based

Table 1: Recent fire losses in large warehouse storage facilities

5/22/2009	Furniture Warehouse – Houston, TX	$4,600\,m^2$ warehouse, filled with furniture and electronics. An Inventory of $5 million was lost. 120 Fire Fighters were involved in putting the fire out [3].
12/11/2007	Warehouse Fire – Hemingway, SC	$15,329\,m^2$ warehouse storing plastic Tupperware. Warehouse was protected by sprinklers to code, 78 firefighters responded but fire burned out of control for a 35-hour period [1].
6/19/2007	Furniture Warehouse Fire – Charleston, SC	9 firefighters died. Flashover occurred while firefighters were attempting to find the seat of the fire, after one employee was rescued [4].
12/16/2003	Furniture Warehouse Fire – New York	1 firefighter died while searching for the seat of a fire in a furniture and mattress warehouse [5].
3/14/2001	Supermarket Fire – Phoenix, AZ	1 firefighter died. Fire began in storage pile in the rear of the store, spreading throughout the store rapidly via attic and duct space [6].
12/18/1999	Paper Warehouse Fire – MS	1 firefighter died after becoming lost in a paper warehouse fire. The structure was equipped with a sprinkler system [7].
12/3/1999	Cold-Storage and Warehouse Building Fire – MA	6 firefighters died after becoming lost in a six-floor, maze-like building searching for two victims. The building was abandoned at the time of the fire [8].
4/16/1996	Lowe's Store – Albany, GA	Fire grew so rapidly it penetrated the roof and filled the building with smoke down to the 1.5 m (5 ft) level, all within about 5 minutes. The fire took over 2 days to extinguish, destroying the 8,000 m2 warehouse. The fire resulted from commodities stored in racks not matched to the fire hazard [9].

upon full-scale rack storage tests of "standard" commodities. Standard commodities consist of a product, usually plastic, paper, or glass cups contained within a segregated corrugated cardboard box [10]. The Group A plastic commodity whose product consists of all plastic cups represents the greatest fire hazard tested. The classification scheme currently used in the United States classifies commodities into one of seven groups, Class I-IV general commodities or Group A-C plastic commodities. The scheme was developed from large-scale tests, comparing the performance of fire sprinklers with varying water application densities to control a fire in a large rack-storage configuration of commodities [11]. In general, stored commodities for warehouses undergo a variety of small-scale tests as an initial evaluation of their fire hazard, but for even moderately hazardous commodities, additional mid-to-large-scale testing is required at great expense [12]. There does not currently exist a good method to correlate or compare small-scale test data to large-scale fire tests. Attempts to develop a large-scale model have also not addressed the fact that commodities involve several mixed materials, and the influence of these different materials together must be accounted for.

Specific Objectives

Current building codes categorize the hazard of different materials by grouping them by Class I, II, III, IV, or Group A, B, or C classifications. For example, corrugated cardboard would be considered as a Class III commodity whereas polystyrene would be considered as a Group A commodity. This implies that polystyrene is more hazardous and requires more stringent fire protection measures. This classification process may involve estimation or guesswork of which class or group to assign a commodity, especially for newly developed materials or mixed commodities. There has been limited fundamental science to justify any of these test results and therefore each industry or

organization has developed a unique set of test methods to evaluate materials. Although the characteristics that would define the flammability of a material should be universal, the multitude of test methods indicates otherwise. Currently, no tests known to the authors provide a complete set of fundamental, nondimensional parameters that could be used in engineering calculations towards safer design of large storage facilities. The development of such test methods and classification methodology with a fundamental scientific basis may fulfill an urgent need for safer warehouse design methods.

This work was performed in conjunction with small-scale experiments performed by Michael Gollner at the University of California, San Diego [13]. Gollner conducted tests at Worcester Polytechnic Institute (WPI) in 2008 at the small-scale in which a fully packed Group A commodity consisting of 125 polystyrene cups was burned under a large product collection hood. The small-scale test commodity boxes were insulated on all sides except for the front, to isolate burning to the front face only. The commodity was ignited uniformly along the base and the mass-loss rate, pyrolysis height, and flame heights were measured for each test. A method to evaluate commodity fire hazards based on the mass-loss rate of tests was then developed and evaluated for the Group A commodity. This premise motivated the present investigations.

In this study, the B-number was determined experimentally using a bench-scale test method. A fundamental approach to flammability ranking for warehouse commodities is developed and results in a more scalable, simple model by utilizing the dimensionless B-number. The B-number was then input in a flame spread model for corrugated cardboard to predict flame heights at the warehouse scale. Corrugated cardboard was chosen in this analysis because it is usually the first source of flaming combustion to sustain flame spread in a warehouse fire. Polystyrene was chosen as a fuel because it is typically used as the worst-case product in large-scale fire testing.

2 Background

Warehouse storage occupancies continue to increase in size, thereby creating a challenging problem for the fire protection engineering field, the fire service, and existing fire and building codes. Warehouses are reaching heights never before considered by existing fire codes, on the order of 80 to 100 foot (24 to 30 m) high stacks of storage commodity. Over the last 50 years, fire protection engineers have relied on large-scale tests to classify commodities into one of seven classes [14] which are representative of their fire performance under specific geometric configurations and ignition conditions. This classification process may involve estimation or guesswork of which class or group to assign a commodity, especially for newly developed materials or mixed commodities. There has been limited fundamental science to justify any of these test results and therefore each industry or organization has developed a unique set of test methods to evaluate materials. Although the characteristics that would define the flammability of a material should be universal, the multitude of test methods indicates otherwise. Currently, no tests known to the authors provide a complete set of fundamental, nondimensional parameters that could be used in engineering calculations towards safer design of large storage facilities. The development of such test methods and classification methodology with a fundamental scientific basis may fulfill an urgent need for safer warehouse design methods.

A series of recent losses in large, protected warehouses, reviewed in Part I of this paper [15], motivated this study. The negative impacts of these devastating fire incidents were felt by occupants, firefighters, insurance interests, and local environments. From a business aspect, millions of dollars of materials or products are lost and operations may be halted [16]. Furthermore, insurance premiums are increased as a result of the fire and lost time can never be recovered. From a life-safety aspect, the lives of workers and responding firefighters are endangered which can result in injuries or death.

Water runoff from firefighting operations and resulting smoke plumes can also detrimentally affect surrounding environments. The potential for a fire in a warehouse is high due to dense packing and large amounts of flammable materials such as paper, plastic, and packaging materials [17]. Currently, warehouses and storage areas are protected by prescriptive fire and building codes which differ according to the industry. A scientifically-based approach is proposed here in order to quantify the hazards presented by different commodities and available fuels with the goal of designing suppression systems matched to stored commodities in the future.

This study focuses on the initial stage of a warehouse fire, which is characteristic of the time before sprinklers are activated and where the commodity packaging (in this case, single-wall corrugated cardboard) is the source of flaming ignition and fire spread. As the fire grows in size, the stored commodity such as paper, plastics, appliances, or other fuel types within the packaging could become involved with the fire. Figure 1 shows an overview of the different scales inherent in the warehouse fire problem and highlights the scales at which this study approaches the problem. Part I of this paper examined a method to link the results from small-scale testing to large-scale warehouse fires. The small-scale tests involved a Group A plastic commodity which consisted of a single corrugated cardboard box (measuring 53 x 53 x 51 cm) filled with extruded polystyrene cups segregated by corrugated cardboard dividers. This configuration is representative of an industry standard fuel package. One face of the commodity was exposed and ignited resulting in flame heights that reached 70-150 cm in height. A method to evaluate commodity fire hazards based on the mass-loss rate of the tests was then developed and evaluated for the Group A commodity. Part II of this study details a method which can link bench-scale testing results to large-scale warehouse fires by separately analyzing the processes of mass and heat transfer. The bench-scale tests performed in this study involved a small, flat sample (measuring 5 x 20 cm) of corrugated cardboard or polystyrene where burning was isolated to one

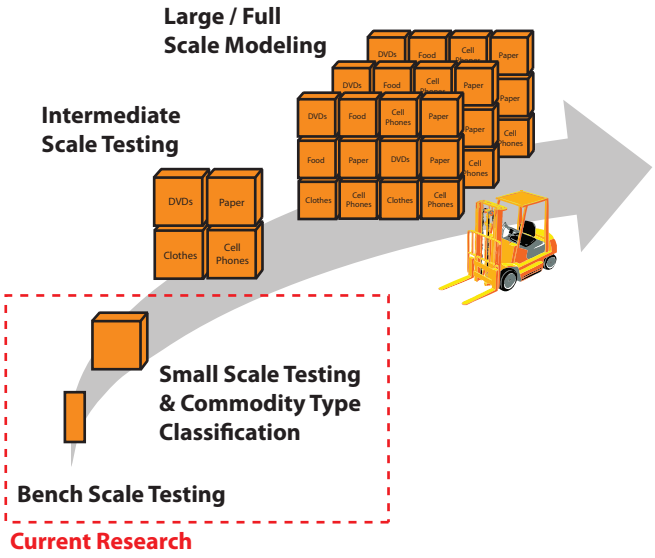

Figure 1: *The warehouse fire problem approach. The scales worked on in this study are shown by the dashed box.*

side and occurred in a laminar fashion. A methodology to calculate a nondimensional mass transfer parameter from bench-scale tests is outlined which captures the effect of commodity material properties on flame spread. A flame spread model was then developed which predicts flame heights in large-scale warehouse configurations as a function of a nondimensional mass transfer parameter and separately accounts for the convective and radiative heat transfer and flow conditions. The nondimensional mass transfer parameter captures the condensed phase pyrolysis phenomena and the heat transfer was evaluated by separately incorporating convective and radiative heat transfer.

3 Literature Review

Numerous studies have attempted to describe the large-scale effects of a warehouse fire by using small-scale test methods for detection and suppression applications. One such effort by Hamins and McGrattan [18] attempted to construct single-cell replicates

of a boxed commodity. The purpose of the small-scale polystyrene and corrugated cardboard tests was to provide input parameters into a fire model in order to numerically model the heat release rate and suppression for a large-scale warehouse fire. The model predictions were then validated against experiments conducted on commodities consisting of Group A polystyrene cups with water being applied above the fire. A correlation between the heat release rate and the water application rate was formed, but it was unable to describe detailed fire growth in storage applications. It also concluded that acquiring input data for materials is a lengthy and costly process, even for a simple geometric configuration.

Another effort by Grant and Drysdale [17] modeled flame spread during the early growth stages of a warehouse fire along corrugated cardboard. They adapted the linearized Satio, Quintiere, and Williams [19] flame spread model with Karlsson's [20] burnout length to be solved numerically. This enabled the flame height, velocity, and pyrolysis front progression to be modeled numerically as a two-dimensional problem. Alvares et al. [21] studied the effects of panel separation on vertical flame spread and mass-loss rates in small-scale corrugated cardboard tests in order to determine fire growth and the effectiveness of sprinkler suppression in warehouse fires.

Continued efforts by Inganson and de Ris [22] and Inganson [23] served to identify the importance of the configuration of the commodities, the mode of heat transfer, and the flue spacing of the commodity boxes in warehouse fires. Inganson's work [22] identified the dominant factors in the warehouse fire growth process, and emphasized the importance of separation of material properties of the fuel from the heat transfer and flow conditions that can result due to the various configurations of the fuel packages. In separating the warehouse fire problem into two distinct phenomena, it then becomes a problem of material properties (condensed phase) and one of the flow conditions and heat transfer (gas phase). Work performed by de Ris and Orloff [24] and

de Ris et al. [25] as well as Foley [26] and Foley and Drysdale [27] served to characterize the mode of heat transfer on an upward propagating flame in a warehouse configuration and quantify the convective and radiative heat transfer that drives the upward flame spread process in the gas phase. Variations in heat transfer from the small-scale to the large-scale was shown by de Ris et al. [25] to be related by similarity effects present in buoyant, turbulent boundary layer flows. This effectively allows analytical results developed for heat and mass transfer in laminar boundary layers to be applied to turbulent boundary layers.

Heat and mass transfer, shape of the fuel surface, and velocity of the air stream are the main driving forces related to fire spread. In a warehouse setting, heat transfer can be in the form of strong convective forces due to tunneling effect of the flue spaces as well as radiation due to large luminous flames. Convective heat transfer depends on the nature of the flow field which can be resolved as a first approximation using classical correlations developed for turbulent boundary layer flows [28]. Radiative heat transfer can be modeled if the soot yield is known accurately. For an engineering application, such as the current study, an elegant approach using the smoke point to correlate soot yield of different fuels was developed by Markstein and de Ris [29]. More theoretical and experimental studies of this problem are needed.

In the early stages of a warehouse fire, before the fire sprinklers activate, mass transfer is intrinsically coupled to material properties of the stored commodity, packing material, and the outer corrugated cardboard covering. Owing to the different burning behavior of each material, which is also a function of the packing and orientation, the problem of classifying a commodity based on its fire hazard is significantly complicated. A general approach to heat, mass, and momentum transfer by way of differential equations for simple geometries such as droplet, flat horizontal, and vertical plate are discussed extensively in fire literature [30–33]. Physically, all of these theories rely

on the Reynolds analogy extended to include combustion of solid fuels [34] in the form:

$$\frac{\tau}{U\nu^{2/3}} = \frac{h}{c\alpha^{2/3}} = \frac{\dot{m}''}{D^{2/3} \cdot \ln(1+B)}. \tag{1}$$

Equation 1 is also referred to as the Chilton-Colburn [35] extension to Reynolds analogy, since it incorporates both turbulent as well as laminar molecular processes of diffusion (ν = kinematic viscosity or momentum diffusivity, α = thermal diffusivity, D = species diffusivity). Equation 1 implies that the shear stress at the surface (τ) is related to the heat transfer (h/c) and mass transfer $(\dot{m}'')$. U, h, and c are the free stream velocity, heat transfer coefficient, and specific heat of the gas, respectively. "B," appearing in Eq. 1 is a nondimensional proportionality constant relating the rate of mass transfer (vaporization, combustion) to the heat transfer and shear stress. A recent study by Raghavan et al. [36] further analyzes this proportionality and shows that Eq. 1 is valid except during ignition and extinction conditions. Since the B-number in Eq. 1 is used in an expression for driving forces, it is also called as a "transfer number" by Spalding [37] and is typically represented [38] as:

$$B = \frac{(1-\chi)Y_{O_2,\infty}(\Delta H_c/r) - c_p(T_p - T_\infty)}{\Delta H_g + Q}, \tag{2}$$

where χ is the fraction of radiation lost to the environment, $Y_{O_2,\infty}$ is the mass fraction of oxygen in air, ΔH_c is the heat of combustion, r is the mass consumption number given by $(Y_{O,\infty}/\nu_s)$, c_p is the specific heat of air, T_p is the vaporization temperature of the fuel, T_∞ is the ambient temperature, ΔH_g is the heat of gasification, and Q represents the energy losses at the fuel surface.

Since B is composed of material-related properties (2), it has been used to rank material flammability in fire literature [39–42]. Figure 2 shows the variation of the B-number for a range of fuels [41] as a function of pyrolysis temperature. The circles

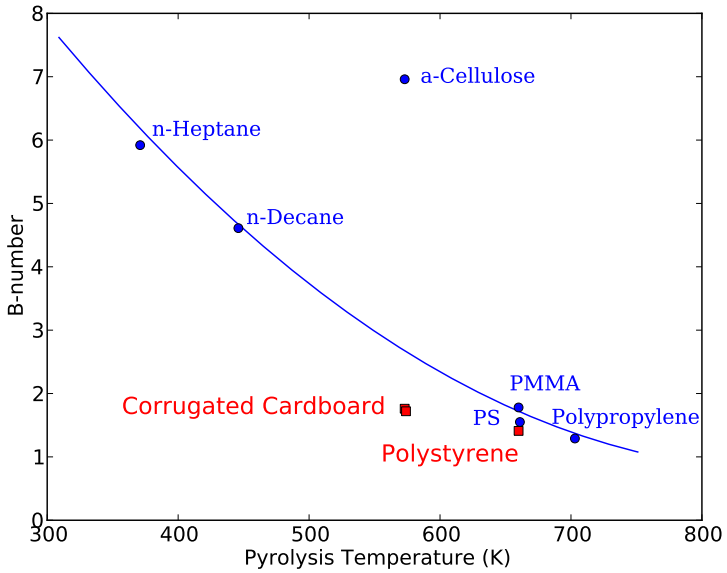

Figure 2: *Values of the B-number for a range of fuels. The circles are B-number values from Annamalai and Sibulkin [41] which were calculated using thermodynamic properties only. The red squares show the B-number values obtained experimentally by this study.*

show the values of the thermodynamic B-number (Eq. 2) versus the pyrolysis temperatures for fuels as calculated by Annamalai and Sibulkin [41]. The thermodynamic values of the B-numbers are calculated using Eq. 2 where χ and Q are assumed to be equal to zero, which represents an ideal value for which there are no losses. The liquid fuels have a larger B-number value and a lower pyrolysis temperature, which corresponds to a smaller amount of energy required to gasify liquid fuels versus solid fuels. In general, a lower B-number indicates a higher pyrolysis temperature, as the fuel will require more energy to gasify. Whereas a higher B-number indicates a fuel with a higher thermodynamic efficiency during combustion [13].

A simple form of mass transfer is derived by rearranging Eq. 1 for the mass-loss rate to yield the expression

$$\dot{m}'' = \frac{h}{c} \ln(1 + B) \tag{3}$$

with the assumption $\alpha = D$ and $Le = 1$ will be used to determine a B-number for a

given fuel by measuring the mass-loss rate experimentally. More exact functions of B than $\ln(1+B)$ can be derived in particular cases by solving the typical differential equation and boundary condition for mass transfer. Expressions for the burning rate of a droplet [30, 43], flat horizontal plate [31], vertical plate [31–33] have been developed in fire literature. Most importantly, all expressions relate the mass burning rate as a function of the B-number. A simple form of mass transfer such in Eq. 3 was chosen in this study because the expression follows directly from Reynolds analogy, and is easily implemented in an engineering test methodology towards warehouse commodity classification.

This study emphasizes that the B-number is primarily a function of the material properties of a given fuel and it can be obtained in a controlled experimental environment by assuming that the primary mode of heat transfer for upward flame spread at the bench-scale is convection [44]. Therefore, the experimental calculation of the B-number will focus on the dominant mode of heat transfer as laminar, natural convective heat transfer to a vertical plate. In examining Eq. 2, it is seen that the B-number can be considered as a ratio of available energy (heat of combustion) to the energy required to gasify a given fuel (heat of gasification). Thus the B-number is intrinsic to the properties of the material and is independent of scale, allowing the results from the bench-scale tests to be used to predict flame heights in large-scale warehouse fires.

4 Experimental Setup and Observations

Figure 3 shows a schematic of the experimental setup. A total of 14 tests were performed with 3 different samples consisting of single-wall corrugated cardboard, polystyrene, and single-wall corrugated cardboard backed with polystyrene. The samples measured 5 cm wide by 20 cm in height; this aspect ratio was chosen as laminar flame

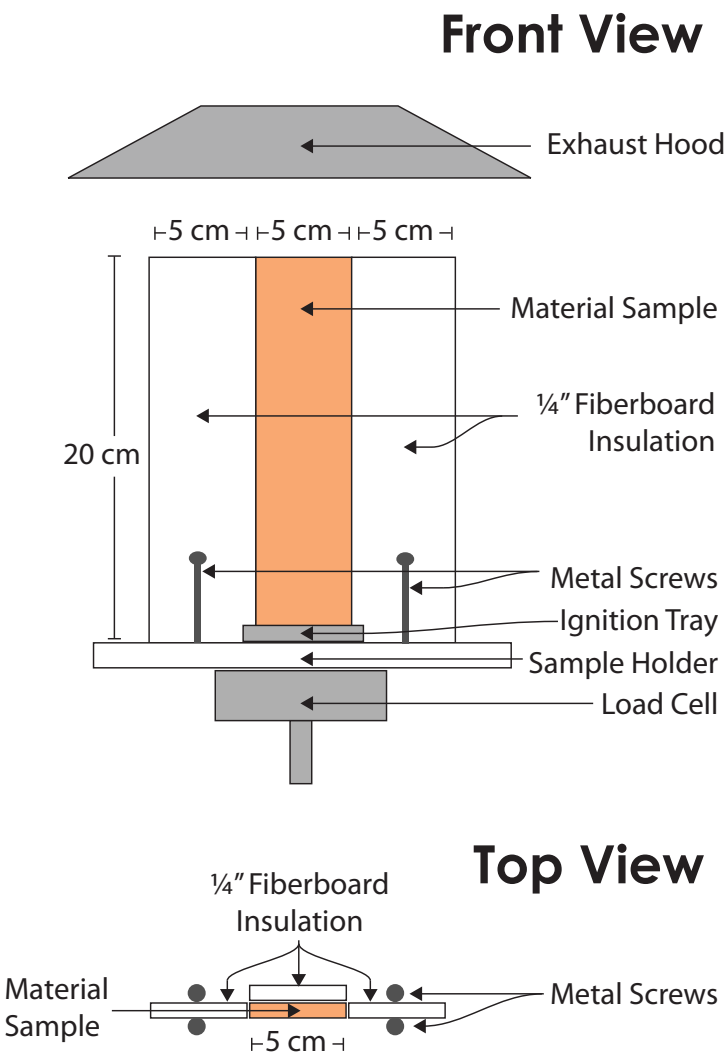

Figure 3: *Schematic of experimental setup.*

spread was the primary focus of this study and upwardly-spreading flames typically become turbulent above 20 cm [45]. The typical mass of the samples was 4 g for corrugated cardboard and 36 g for polystyrene. Corrugated cardboard was chosen as a fuel because it is usually the first item to ignite and sustain flame spread in a warehouse fire. Polystyrene was chosen as a fuel because it is typically used as the worst-case product in large-scale fire testing. The sample which consists of corrugated cardboard backed by polystyrene was chosen as it is representative of a packed or mixed commodity which consists of both corrugated cardboard packaging and polystyrene material contained within. The measured quantities for each test include the mass-loss rate, flame height, and pyrolysis height.

The corrugated cardboard used in these tests was identical to the configuration and thickness that is used to package standard large-scale test commodities and of the same type used in the small-scale tests that were performed by the authors in Part I [13]. The corrugated cardboard samples were type 'C' flute with a nominal thickness of 4 mm and 135 flutes per meter width [46] as shown in Figure 4(a). All tests were performed with the flutes aligned vertically along the 20 cm dimension, which is similar to the orientation of the flutes in an upright commodity box. The polystyrene samples were 3 mm thick as shown in Figure 4(b).

The mode of ignition for the tests was a small aluminum tray (Figure 3) placed at the base of the sample measuring 5 x 0.5 x 0.5 cm which contained a thin strip of glass fiber insulation soaked with heptane. This ensured a uniform mode of flaming ignition along the base of the fuel sample. The corrugated cardboard tests used 0.25 mL of heptane for ignition while the polystyrene tests used 0.75 mL of heptane, as it took a longer time for the polystyrene samples to ignite.

The vertical fuel samples were insulated on the back and sides with 0.25 inch (0.64 mm) thick fiberboard insulation to isolate burning to the front face of the samples only.

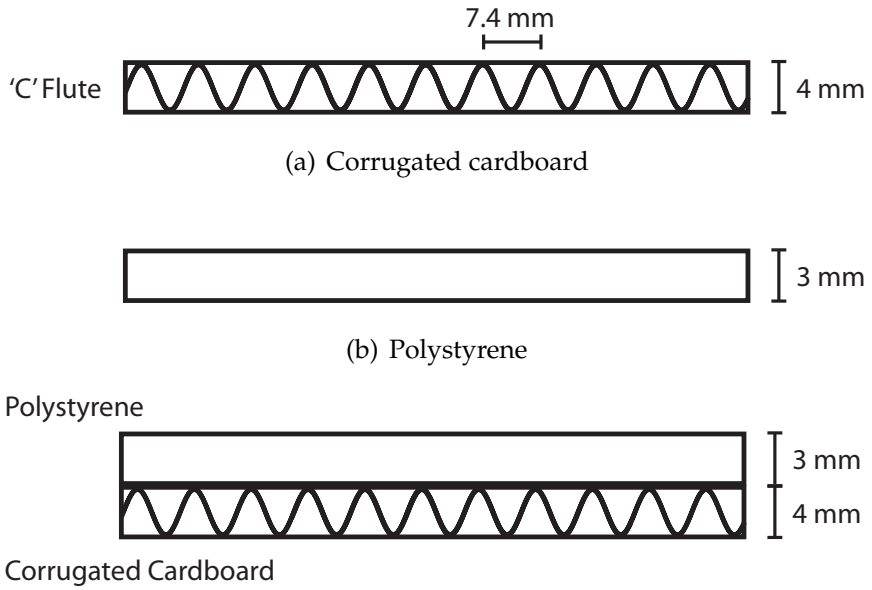

(a) Corrugated cardboard

(b) Polystyrene

(c) Mixed fuel - corrugated cardboard backed with polystyrene

Figure 4: *Cross-sectional detail of: (a) Corrugated cardboard samples used in tests. The paper sheets are of a 26-26-26 lb. basis weight. (b) 4 mm thick polystyrene sheets used in tests. (c) Mixed-commodity sample (corrugated cardboard backed with polystyrene) used in tests.*

The samples were held in by the insulating fiberboard sheets which were supported by four metal screws attached to the 0.75 inch (1.9 cm) thick fiberboard base (Figure 3). All of the corrugated cardboard tests burned to completion and self-extinguished once the fuel was depleted. The polystyrene samples were manually extinguished after the flame had reached a pyrolysis height of about 10 cm due to excessive smoke production and dripping. The dripping and deformation of the polystyrene was not considered to be significant during the time period of upward flame spread considered in the results since the sample size in the experiment was small and significant accumulation of melted polystyrene was not observed.

The mass lost by the specimen was measured continuously using a load cell (Automatic Timing & Controls model 6005D) with an accuracy of $\pm$ 0.5 g as specified by the manufacturer. This is approximately 12% of the nominal initial mass of the corrugated cardboard samples and 2% of the nominal initial mass of the polystyrene samples. The

load cell was calibrated prior to each test series using standard test weights. To measure flame heights and record the burning history of the tests, video and still images were captured using a Sony Handycam HRR-SR5 model camera and a Canon EOS-5D digital single-lens reflex (DSLR) camera. Figure 5(a) depicts a visual time history of vertical flame spread along the corrugated cardboard sample and Figure 5(b) depicts vertical flame spread along the polystyrene sample. The images were then loaded onto a PC and a custom MATLAB image processing script was used to extract the flame heights as a function of time from each test. The flame height was defined as the tip of an attached yellow flame, and the computer-processed images were consistent with visual measurements of the video.

To obtain pyrolysis heights for the corrugated cardboard samples, thermocouples (Omega model 5TC-GG-K-30-36) were instrumented on the inside of the front face of the corrugated cardboard layer and an ignition temperature of 380° C was used to determine the location of the pyrolysis front as a function of time. This was combined with observations of the visual charring on the corrugated cardboard to verify the location of the pyrolysis height. For the polystyrene, visual bubbling and charring from the video was used to determine the location of the pyrolysis front. Since the corrugated cardboard and polystyrene tests were found to be repeatable and the pyrolysis front in the laminar regime were non-accelerating, a linear approximation of the pyrolysis heights was made. This approximation was later used to determine an average mass-loss rate per unit area, and finally, the B-number for each test. The fit was generated using a constant upwards flame spread velocity up to 20 cm for corrugated cardboard (total involvement of the sample) or 10 cm for polystyrene (maximum pyrolysis height attained in polystyrene tests). After this maximum pyrolysis height was reached, a constant height of 20 cm (corrugated cardboard) or 10 cm (polystyrene) was assumed. Figure 6 shows the pyrolysis height data fit used to determine the B-numbers for the corrugated cardboard samples. Details on the polystyrene pyrolysis

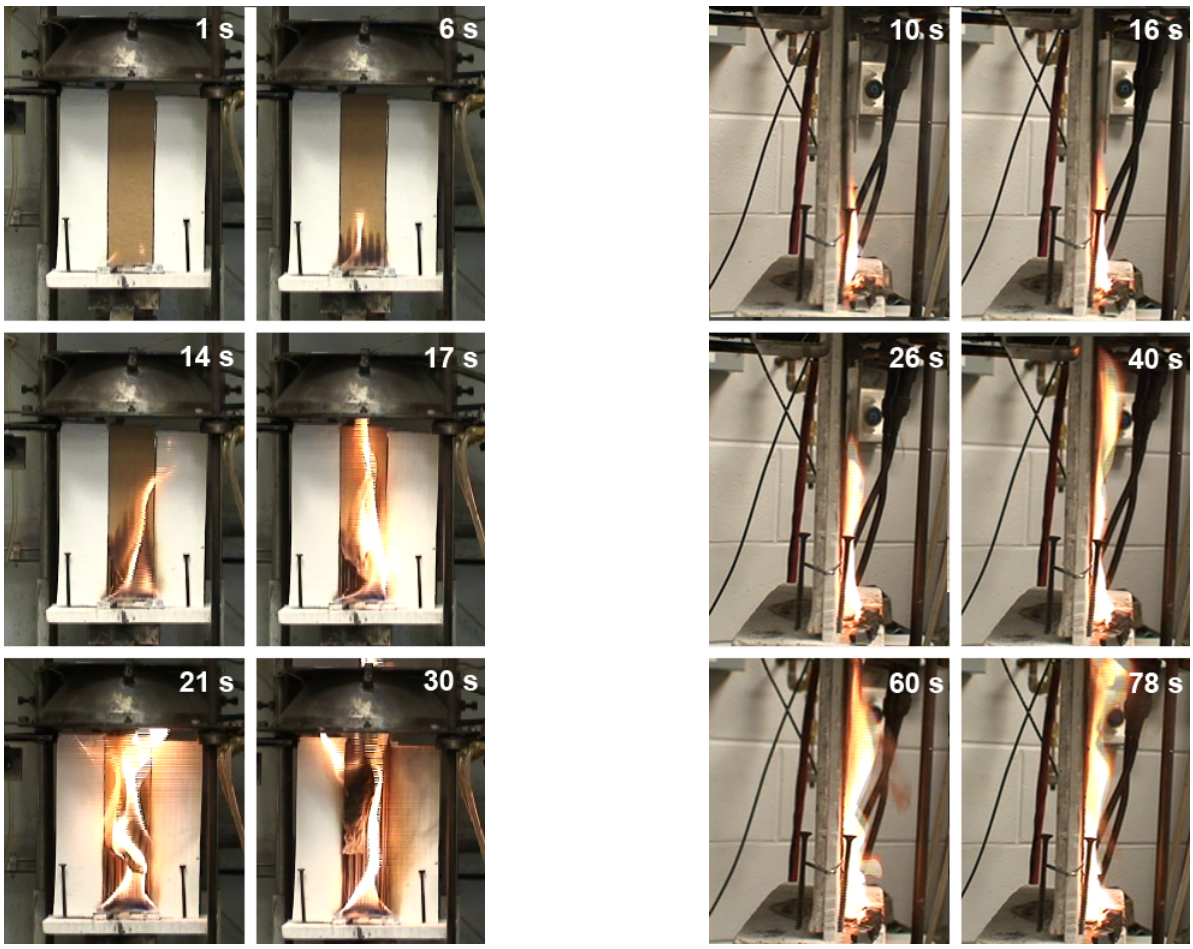

(a) Corrugated cardboard (b) Polystyrene

Figure 5: *Illustrated time history of flame heights from bench-scale tests. (a) Front view of corrugated cardboard. (b) Side view of polystyrene.*

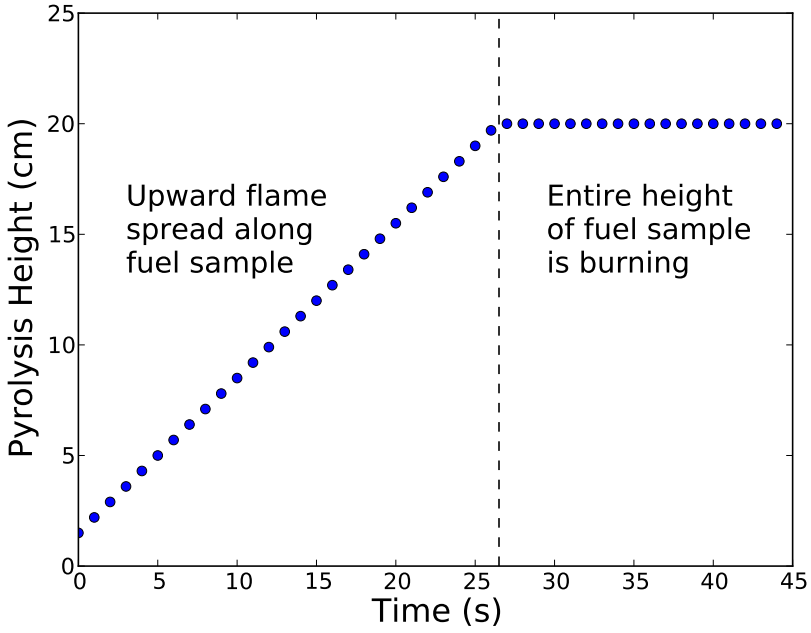

Figure 6: *Pyrolysis height data fit from corrugated cardboard tests.*

height data fits can be found in Overholt [47].

The B-number was then determined by the following method. The mass-loss rate data was trimmed to contain only the time period where upward flame spread occurred along the sample. This was achieved by reviewing the video recording as well as mass-loss data for a particular test. Figure 7 shows an example of the mass-loss rate from one of the tests and the trimmed portion used to determine an average mass-loss rate per unit area. After the mass-loss rate was trimmed, it was then divided by the time-dependent pyrolysis height and multiplied by the width of the sample to obtain an average mass-loss rate for each test. For example, the average mass-loss rate per unit area of a 5 cm wide corrugated cardboard from a sample test was found to be $7.7 \cdot 10^{-4}\ g/cm^2 s$. The average mass-loss rate value was then input into the experimental B-number formulation given by

$$B = \left(\frac{\dot{m}''_f}{\rho_g \alpha_g 0.59 / x_p [g x_p \beta \Delta T / \alpha_g \nu_g]^{1/4}} \right) - 1, \tag{4}$$

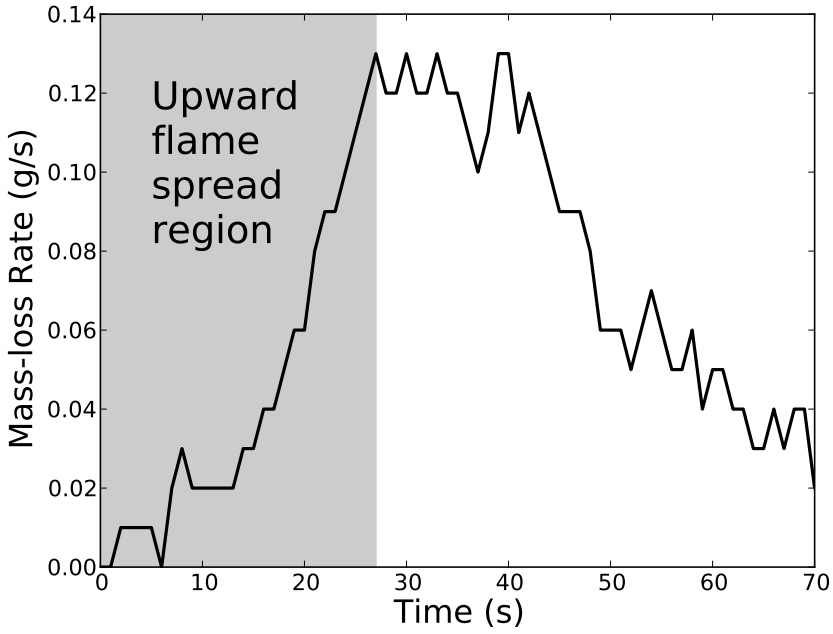

Figure 7: *Mass-loss rate for a corrugated cardboard test. The shaded region shows the trimmed portion of the mass-loss rate during upward flame spread.*

which uses a standard heat transfer coefficient for laminar, natural convective flow over a vertical plate, where $\dot{m}''_f$ is the average mass-loss rate, ρ_g is the density of air, α_g is the thermal diffusivity of air, x_p is the pyrolysis height, g is the acceleration due to gravity, β is the thermal expansion coefficient given by $1/T_m$, $\Delta T = T_m - T_\infty$, and ν_g is the kinematic viscosity of air. A mean gas temperature, T_m, was used for T_f in the calculations by averaging the temperature of ambient gas, $T_\infty = 20^\circ C$, and an approximate flame temperature for cellulosic materials, $T_f = 800^\circ C$ [48]. Eq. 4 is derived fully in Part I of this paper. Table 2 lists all values used in Eq. 4. The thermo-physical properties of air are estimated at a mean gas temperature (T_m) and are assumed to be constant [49].

Table 2: Properties used in calculating the B-number (Eq. 4) estimated at a mean temperature of 683K [50].

Property	Value
ρ_g	$0.50\ kg/m^3$
α_g	$98 \cdot 10^{-6}\ m^2/s$
Pr	0.7
g	$9.81\ m/s^2$
T_m	$683\ K$
T_∞	$298\ K$

5 Flame Spread Model

Figure 8 shows a schematic of the flame spread model. The pyrolysis zone is defined as the region of the solid fuel which is outgassing combustible fuel vapors up to the pyrolysis height (x_p). Some of the fuel burns directly in front of the fuel surface, while some fuel is carried above its height of origin and burns above, heating the virgin material in the preheat zone (δ) up to its ignition temperature. The fuel carried above the pyrolysis zone is called *excess pyrolyzate* [51] and forms the physical flame height (x_f), which drives the flame spread process. The rate of upward flame spread depends on both the amount of energy released by the combusting fuel and the the rate at which the material pyrolyzes due to the flame heat flux $(\dot{q}''(x))$. This creates a method for energy to feed back from the gas phase to the condensed phase and this feedback loop is what drives the flame spread process. The B-number describes the mass flux from the condensed phase fuel surface and some nondimensional gas phase parameter can be used to describe the heat transfer from the flame, which will be discussed later. In the flame spread model, the heat flux is assumed constant along the pyrolysis region up to the pyrolysis height as $\dot{q}''(x) = \dot{q}''(0)$. In the preheat region (δ), the heat flux is assumed to decay exponentially as a function of the preheat region as $\dot{q}''(x) = \dot{q}''(0)e^{-x/\delta}$. Once the material in the preheat region reaches its pyrolysis temperature, it begins to outgas combustible materials and the pyrolysis region ex-

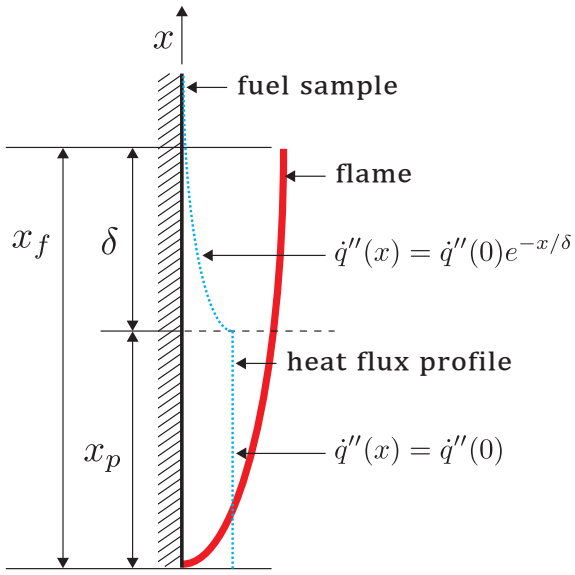

Figure 8: *The upward flame spread model proposed by Sibulkin and Kim [52]. x_p is the pyrolysis height, x_f is the flame height, δ is the preheat distance, and $\dot{q}''(x)$ is the flame heat flux (dotted line).*

pands, resulting in a larger flame height and more energy feedback to the unburned fuel. Therefore, the process of upward flame spread can be considered as a moving ignition front.

Thus, while solving numerically for flame spread, the material sample is discretized into sections measuring 0.1 cm in height and the initial conditions for the pyrolysis height and flame height are input into the model. The heat flux profile is mapped along the height of the sample (as in Figure 8) by using the following boundary conditions at the surface

$$\dot{q}''(x) = \dot{q}''(0)\exp\left(-x/\delta\right) \quad \text{if } x > x_p \tag{5a}$$

$$\dot{q}''(x) = \dot{q}''(0) \qquad \text{if } x \leq x_p \tag{5b}$$

where $\dot{q}''(0)$ is constant but can be modified depending on how the mode of heat transfer is modeled, x is the height along the fuel sample, and δ is the preheat region

$(x_f - x_p)$. Initially, only convective heat transfer was considered in the flame spread model given by the Nusselt correlation detailed in Part I of this paper as

$$h_c = \frac{c_g \rho_g \alpha_g}{x_p} \overline{Nu}_x, \tag{6}$$

where h_c is the convective heat transfer coefficient, c_g is the specific heat of air, ρ_g is the density of air, α_g is the thermal conductivity of air, x_p is the pyrolysis height, and the local Nusselt number is used for natural, laminar convection along a vertical plate as $Nu = 0.59(GrPr)^{1/4}$ [46]. Using this definition for the convective heat transfer coefficient, the initial heat flux, $\dot{q}''(0)$, to be used in Eqs. 5a & 5b is given as

$$\dot{q}''(0) = \dot{q}''_c = h_c(T_m - T_\infty), \tag{7}$$

where h_c is the convective heat transfer coefficient, T_f is the flame temperature, and T_∞ is the ambient temperature. This results in a total flame heat flux where $\dot{q}''(0) = 5.5\ kW/m^2$ for this configuration. A mean gas temperature, T_m, is used for T_f in the calculations by averaging the temperature of ambient gas $(T_\infty = 20^\circ C)$ and an approximate flame temperature for cellulosic materials $(T_f = 800^\circ C)$ [48, 49]. Heat fluxes which incorporate both convection and radiation will be discussed later when considering large-scale warehouse flame spread, which essentially modify the $\dot{q}''(0)$ term in Eqs. 5a & 5b.

After the heat flux is mapped along the height of the sample for the first time step, the forward heating parameter ϕ is calculated and is later used to find the velocity of the pyrolysis front. ϕ was defined by Sibulkin and Kim [52] as the ratio of the forward heating distance to the rate of heat release per unit width of the fuel ($\phi = \dot{q}'_F / \dot{q}'_c$). The forward heating distance $(\dot{q}'_F)$ is calculated by the integral of the heat flux above the

Table 3: Physical properties for corrugated cardboard and polystyrene

Property	Corrugated Cardboard	Polystyrene	Units
k	0.06 [53]	0.12 [41]	$W/m \cdot K$
ρ_s	8.39 [54]	1.07 [41]	g/m^3
c_p	1.20 [54]	1.34 [41]	$J/g \cdot K$
ΔH_c	14,090 [55]	23,610 [55]	J/g
ΔH_g	2,200 [54]	1,590 [54]	J/g
T_p	573 [41]	660 [41]	K

pyrolysis length (x_p) as in

$$\dot{q}'_F = \int_{x_p}^{\infty} \dot{q}''(x)dx, \tag{8}$$

where $\dot{q}''(x)$ is the heat flux along the height of the sample (Eq. 5a) and $\dot{q}'_c$ is the rate of heat release per unit width of the sample given by $\dot{q}'_c = \dot{m}'_f \Delta H_c$. An expression for the mass flux from the pyrolysis region $(\dot{m}'_f)$ obtained by Sibulkin and Kim [52] is given by

$$\dot{m}'_f(x_p) = 0.59 \frac{\mu_f}{Pr^{3/4}} \left(\frac{g\beta\Delta T}{\nu_g} \right)^{1/4} \ln(1+B) x_p^{3/4} \text{ (laminar)}, \tag{9a}$$

$$\dot{m}'_f(x_p) = 0.13 \frac{\mu_f}{Pr^{2/3}} \left(\frac{g\beta\Delta T}{\nu_g} \right)^{1/3} \ln(1+B) x_p^{3/4} \text{ (turbulent)}, \tag{9b}$$

where μ_f is the viscosity of air, Pr is the Prandtl number, g is acceleration due to gravity, β is the thermal expansion coefficient, ΔT is defined as $(T_m - T_\infty)$, ν_g is the kinematic viscosity of air, B is the B-number for the material as found by Eq. 4, and x_p is the pyrolysis height. The flame spread model switches to the turbulent formulation when the flame height (x_f) becomes greater than 20 cm in length [45]. Once ϕ is calculated from $\phi = \dot{q}'_F / \dot{q}'_c$, the velocity of the moving pyrolysis front for the current time step is found by

$$V(x_p) = A_l \phi x_p^{1/2} \text{ (laminar)}, \tag{10a}$$

$$V(x_p) = A_t \phi x_p \text{ (turbulent)}, \tag{10b}$$

where the terms A_l and A_t are given by

$$A_l = \frac{\Delta H_c \Delta H_g}{(4/3)\rho_s c_s k_s (T_p - T_\infty)^2} \left[0.59 \frac{\mu_f}{Pr^{3/4}} \left(\frac{g\beta_f \Delta T}{\nu_g^2} \right)^{1/4} \ln(1+B) \right]^2 \text{ (laminar)}, \quad (11a)$$

$$A_t = \frac{\Delta H_c \Delta H_g}{\rho_s c_s k_s (T_p - T_\infty)^2} \left[0.13 \frac{\mu_f}{Pr^{2/3}} \left(\frac{g\beta_f \Delta T}{\nu_g^2} \right)^{1/3} \ln(1+B) \right]^2 \text{ (turbulent)}, \quad (11b)$$

where ΔH_c is the heat of combustion, ΔH_g is the heat of gasification, ρ_s, c_s, and k_s are thermophysical properties of the condensed phase, T_p is the pyrolysis temperature of the condensed phase, and the remaining terms are defined in Eqs. 9a & 9b. Table 3 lists the condensed phase properties for corrugated cardboard and polystyrene that are used in Eqs. 11a & 11b.

The resulting velocity of the pyrolysis front is added to the current pyrolysis height for the next time step as $x_p[t + \Delta t] = x_p[t] + V[t] \cdot dt$. For the final part of the time step, the pyrolysis height is converted to a physical flame height by an expression by Annamalai and Sibulkin [40] for natural convection as given by

$$x_f = 0.64(r/B)^{-2/3} x_p. \quad (12)$$

where r is the mass consumption number given by $(Y_{O,\infty}/\nu_s)$ and B is the B-number for the material. This assumption of a constant flame height to pyrolysis height ratio is based on the simplification that the burning rate is a function of the incident heat flux and that all of the excess fuel above the pyrolysis region is burned [40, 51]. After the flame height (x_f) is found, the numerical routine continues to the next time step and repeats starting from Eqs. 5a & 5b. This results in the prediction of flame height as a function of time.

To predict flame heights in the large-scale warehouse fires, both convection and ra-

diation are incorporated into the flame spread model, which effectively modifies the $\dot{q}''(0)$ term in Eqs. 5a & 5b. The simplest method for incorporating radiation is to use the Stefan-Boltzmann equation [46] to represent the radiant heat transfer from the gas phase by adding a radiative component to Eq. 7, resulting in

$$\dot{q}''(0) = \dot{q}_c'' + \dot{q}_r'' = h_c(T_m - T_\infty) + \epsilon\sigma(T_m^4 - T_\infty^4), \tag{13}$$

where $\dot{q}_c''$ is the convective heat flux, $\dot{q}_r''$ is the radiative heat flux, ϵ is the emissivity of the fuel assumed to be unity, and σ is the Stefan-Boltzmann constant $(5.67 \cdot 10^{-8}\ W/m^2 \cdot K^4)$. This results in a total flame heat flux, $\dot{q}''(0) = 17\ kW/m^2$.

A more detailed and useful method for representing radiation in a large-scale warehouse setting is to incorporate a radiant heat-flux correlation based on work by de Ris and Orloff [24] for radiant heat transfer between parallel panels. This expression is useful at the warehouse scale in which flame spread can be considered to be occurring between two parallel plates represented by the flue space between rows of stored commodities. Following the method of de Ris and Orloff [24], the radiant heat flux is calculated using

$$\dot{q}_r'' = \left(\frac{\varsigma_p \dot{q}_A''' w^2 d}{2 x_f w}\right) + \dot{q}_{loss}'', \tag{14a}$$

$$\text{and } \varsigma_p = \frac{\beta_1 (Y_s + Y_g)^{1/4} \varsigma_f}{\varsigma_f + \alpha_p \varsigma_f + \alpha_p} - \frac{2\beta_2 \dot{q}_{loss}''}{d\dot{q}_A'''} \tag{14b}$$

where ς_p is the nondimensional panel width defined as $\varsigma_p =$, $\dot{q}_A'''$ is the volumetric heat release rate assumed to be $1110\ kW/m^3$ [24], w is the sample width, d is the separation distance of the panels, x_f is the flame height, $\dot{q}_{loss}''$ is the surface heat loss rate fixed at a constant value of $5\ kW/m^2$ [24], and β_1 and β_2 are constants equal to 1.04 and 1.7, respectively. Y_s is the soot yield of the fuel and Y_g is added to the soot yield to account for radiation from the combustion gases for fuels having little to no soot and is equal

to 0.01 g/g. ς_f is the nondimensional flame height equal to x_f/w and α_p is the aspect ratio equal to d/w. It should be noted that in this formulation for the radiant heat flux, the space between the panels is assumed to be fully occupied by flames and so an increase in panel separation distance (d) results in an increased radiant heat flux. Thus, the separation distance for this study was fixed at 0.15 m (6 inches) which is representative of the flue space present in a typical warehouse commodity fire test. This expression for the radiant heat flux is dependent on both the flame height and the soot yield of the fuel, which are both important factors to consider when modeling flame spread at the warehouse scale. In this study, a representative value for the soot yield (Y_s) is chosen as 0.01 g for a cellulosic material such as corrugated cardboard which is a very low sooting fuel. The soot yields are assumed to be constant. However, using more information on the smoke point of the fuel from the bench-scale experiments, a variable soot yield can also be implemented. Using the result from Eqs. 14a & 14b for the radiant heat flux, a final expression for the flame heat flux is given by

$$\dot{q}''(0) = h_c(T_m - T_\infty) + \left(\frac{\varsigma_p \dot{q}'''_A w^2 d}{2x_f w}\right) + \dot{q}''_{loss}. \tag{15}$$

and results in a total flame heat flux, $\dot{q}''(0) = 27\ kW/m^2$.

Further analysis on the controlling parameters dominating the heat flux at various stages of the commodity burning is important for future research. The heat flux is a vital part of the problem since it incorporates both geometry (flue spacing, storage height, etc.) and orientation (vertical, horizontal, and ceiling flame spread). Further considerations could be made on the modeling of heat flux to the fuel with an increased level of detail of the geometry and flow conditions. Since we have separated the problem into two parts, material properties and heat transfer, the flow conditions in more complex geometries could be modeled by a computational fluid dynamics code while the B-number would handle the pyrolysis rate of the fuel.

6 Results and Analysis

The results described in this section are based on a total of 14 bench-scale tests that were carried out using samples of corrugated cardboard, polystyrene, and corrugated cardboard backed by polystyrene as discussed in Section 4. After initial ignition along the base of the samples, the flame was observed to spread uniformly in the upward direction along the fuel samples. As the excess pyrolyzate combusted above the pyrolysis zone, the unburned fuel above the pyrolysis zone (x_p) was heated to its ignition temperature and the flame spread upwards at an increasing rate [51]. As described in Section 4, the mass-loss rates were trimmed to only contain the portion of upward flame spread along the sample as described in Section 4.

During the period of upward flame spread, the average mass-loss rate per unit area for corrugated cardboard was within a range of $7.4 - 7.8 \cdot 10^{-4}\ g/cm^2s$ and for polystyrene was within a range of $6.6 - 6.8 \cdot 10^{-4}\ g/cm^2s$. From the average mass-loss rates, a B-number was calculated for each test by using Eq. 4. Using an average value from all tests performed on a given material sample, the B-number for corrugated cardboard was 1.7 (std. deviation of 0.06) and for polystyrene was 1.4 (std. deviation of 0.02). The B-numbers were then input into the flame spread model as described in Section 5 to predict flame heights for both the bench-scale and large-scale cases.

The case of a mixed commodity was also tested to see if the effects of mixed-material interactions could be captured by the bench-scale method. For the mixed commodity tests, 4 samples consisting of corrugated cardboard backed by polystyrene were ignited using the same procedure as the single fuel tests. The experimental setup in this case is considered to be representative of a commodity configuration in which a Group A plastic such as polystyrene is encased by corrugated cardboard. The 4 tests exhibited nearly the same rate of upward flame spread as the tests consisting only of

corrugated cardboard. Therefore, the data fit for pyrolysis height versus time for corrugated cardboard as shown in Figure 6 was used to calculate an average mass-loss rate per unit area for the mixed samples. For the 4 tests conducted in this configuration, the energy from the burning corrugated cardboard was not sufficient enough to ignite the polystyrene before the corrugated cardboard sample was burned away. The mass-loss rates versus time for the 4 mixed commodity tests are shown in Figure 9. The average mass-loss rate per unit area for these tests was within a range of $5.5 - 10.0 \cdot 10^{-4}\ g/cm^2s$. The resulting time-averaged B-numbers for the 4 mixed fuel tests were 1.0, 1.7, 2.7, and 1.3 for tests 1, 2, 3, and 4, respectively. It is hypothesized that the tests with relatively larger B-number values of 1.7 and 2.7 were a result of some gasification of the polystyrene material due to energy contributed from the combusting corrugated cardboard sample. This was observed at the conclusion of the tests as the polystyrene had visually charred or slightly melted onto the corrugated cardboard sample. Whereas the tests with relatively lower B-number values of 1.0 and 1.3 may have been a result of energy lost to the polystyrene sample without significant gasification of the plastic. Future tests can be instrumented with thermocouples to measure the heat loss between the corrugated cardboard and the polystyrene sample and the heat loss from the back of the polystyrene sample. This can lead to further understanding of the process of energy transfer that occurs when heterogeneous materials are burning as a mixed commodity.

The flame spread model was validated at the bench-scale by comparing the results from the model against observed flame heights from the video data for all 14 of the tests. Figure 10(a) shows the flame heights for corrugated cardboard as predicted by the model versus the bench-scale flame heights from the experiments. The flame height predictions for corrugated cardboard are in good agreement with the experimental flame heights. Figure 10(b) shows the flame heights for polystyrene as predicted by the model versus the bench-scale flame heights from the experiments. The

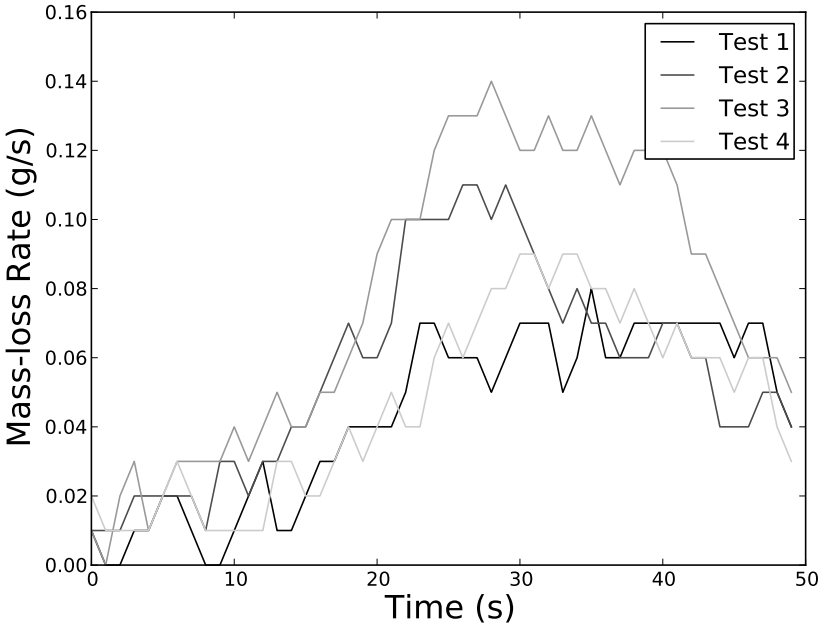

Figure 9: *Mass-loss rates vs. time for 4 tests consisting of corrugated cardboard backed with polystyrene.*

flame height predictions for polystyrene are in good agreement with the experimental flame heights at the bench-scale. The bench-scale predictions are in reasonable agreement with the experimental flame heights since the dominant mode of heat transfer in the tests was assumed to be laminar, natural convection on a vertical plate, and the same mode of heat transfer is assumed in the flame spread model as shown in Eq. 7.

The flame spread model was then validated at the large-scale by comparing flame spread model predictions to flame heights in rack-storage warehouse fire tests. Flame heights for large-scale warehouse fires were obtained from video data from 3 large-scale warehouse commodity fire tests that were performed at Underwriter's Laboratory in Northbrook, Illinois [56]. The fuel consisted of paper cups (Class III commodity) as seen in Figure 11(a) which were packed in corrugated cardboard boxes and stacked between 20 and 30 feet in height (6.1 m to 9.1 m) in a rack-storage configuration. The boxes were ignited along the bottom edge in the flue space between the

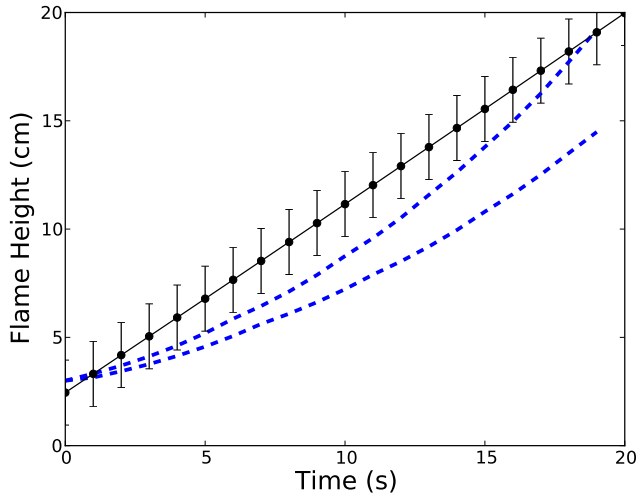

(a) Corrugated cardboard

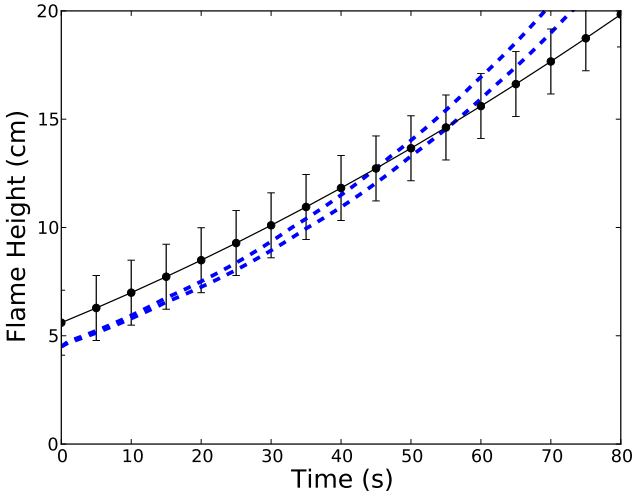

(b) Polystyrene

Figure 10: *Flame heights in the bench-scale tests are compared to the predicted flame heights. The black line shows the measured flame heights with error bars depicting the experimental range. The dashed line shows the upper and lower range of predicted flame heights for the experimental B-number uncertainty where B ranges from 1.61 to 1.73 for corrugated cardboard and from 1.38 to 1.44 for polystyrene.*

racks. Flame height data as a function of time was acquired from the videos. Figure 11(b) shows a snapshot from a warehouse fire test as the flame spreads up through the flue space between the boxes. The flame spread model predictions for flame height were validated against a range of experimental flame heights from 3 large-scale UL tests and the results are shown in Figure 12. The B-number for corrugated cardboard (1.7) was used in the large-scale flame spread predictions since it is nondimensional and describes the mass flux for both the bench-scale and large-scale scenarios. Prior studies have shown that the B-number is not constant, but varies to some degree in both time and space [38]. For the purposes of the large-scale flame height predictions, the B-number was assumed to have a constant value of 1.7. For the gas phase heat transfer, in order to account for radiative effects that are present in the large-scale, 3 different methods for representing the flame heat flux ($\dot{q}''(0)$) are used in the flame spread model as described in Section 5. The flame heat flux which yields the best flame height predictions accounts for both convective and radiative heat transfer by using a radiation correlation based on heat transfer between two parallel plates as shown in Eq. 14a. This is most representative of the fire conditions in the large-scale warehouse fire tests since the fire is ignited in the flue space between the commodity boxes and spreads upwards between the stack of commodity boxes. In this case, radiant energy feedback was occurring between the parallel fuel surfaces and thereby increasing the total heat flux and the flame spread rate accordingly.

7 Conclusions

This work has developed a bench-scale method to experimentally determine the B-number in order to rank the flammability hazard of a given material. The results from the bench-scale tests were then used to model vertical flame spread at the warehouse scale up to 30 feet (9.1 m) in height. The flame spread model showed the best

(a) (b)

Figure 11: *Figure (a) shows the contents of a Class III commodity consisting of paper cups separated by corrugated cardboard partitions. This was the fuel type used in the large-scale warehouse fire tests at UL [56]. Figure (b) shows a snapshot from a warehouse fire test as the flame spreads up through the flue space between the packed commodity boxes.*

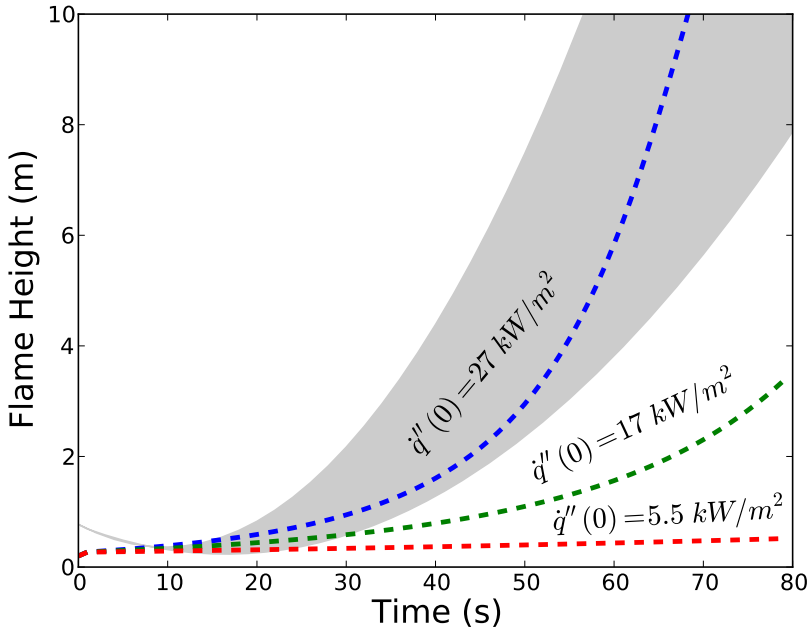

Figure 12: *Flame heights from the large-scale UL experiments are compared to the predicted flame heights using 3 different heat flux models. The flame heat flux value is shown next to the flame height prediction. The gray band shows the range of flame heights as measured from experiment; the dashed line shows the predicted flame heights.*

agreement with the large-scale experimental flame heights (Figure 12) by using the B-numbers that were determined experimentally from the bench-scale tests and the flame heat flux which incorporates both convective heat transfer and a correlation for radiative heat transfer between parallel plates. Therefore, the processes of heat transfer (flow conditions) and mass transfer (B-number) were successfully decoupled and able to be expressed independently of one another, which enabled the scaling of the results from the bench-scale to the large-scale warehouse conditions. The B-number was obtained from bench-scale experiments where the flow conditions can be controlled and thus separated from the effects of material properties. Three different flow conditions were used to model heat transfer in the large-scale and validated by using large-scale commodity fire test data.

It was also shown that since the soot yield (Y_s) is nondimensional and intrinsic to a given material, it can be a useful parameter to model radiation effects at the large-scale. As Y_s increases, the radiant feedback from the gas phase combustion to the fuel increases and this results in an increased rate of flame spread. These two parameters, the B-number and Y_s, can both be determined from bench-scale test methods and utilized in a flammability ranking scheme which is valid in large-scale fires. This establishes the framework for a more cost-effective means to determine the flammability hazard of various commodity materials using a simple bench-scale test method. The B-number was also measured for a sample of corrugated cardboard backed by polystyrene, which is representative of a mixed commodity. As a first estimation of the influence of commodity within corrugated cardboard packaging, the B-number calculated for the mixed sample was discussed. This relates to the objective of the experimental method to determine a quantified flammability ranking for materials consisting of both homogeneous and mixed commodities. More understanding of the physical interaction between multiple material samples is needed in order to quantify the effects of a mixed commodity on the overall flame spread process. A framework

was demonstrated for which the results from bench-scale tests can be used to quantitatively rank the flammability of both single fuels and mixed commodity configurations and predict flame heights at the large-scale. The B-number and soot yield are fundamentally robust parameters that may be used in the future as means to classify the flammability of a given warehouse commodity, to strengthen the level of confidence in ranking a commodity, and to increase the effectiveness of warehouse fire protection and suppression applications.

8 Future Work

A method for experimentally determining the B-number in order to rank the fire hazard of a material using a bench-scale method has been shown and a model for predicting vertical flame spread along corrugated cardboard has been presented. 14 tests were performed as described in Section 4, which describes the experimental setup and mode of burning required for a test to be considered usable for the calculation of the B-number. Uncertainty in the determination of the B-number may be a result of spurious fluctuations in mass loss data during the test burns as well as the mode of burning of the sample. More tests can be performed using the method presented to to increase the confidence in the B-number for a given material. The calculation of the B-number is dependent on the mass-loss rate, therefore, caution should be taken during the bench-scale tests to ensure minimal experimental error occurs which might cause spurious fluctuations to be recorded by the load cell. This could occur due to drafts in the experimental environment or shifting of the fuel sample. The mode of burning along the sample is also important due to the assumed mode of heat transfer for the bench-scale sample as convective, natural convection. Thus, the burning should occur uniformly along the sample in the upward direction, since uneven or horizontal burning or excessive peeling of the samples may result in additional uncertainty in the calculation of the B-number. The design of future sample holders could be improved to better secure the fuel sample in case it deforms or shifts during the tests.

The flame spread model shows good agreement with the large-scale experimental flame heights (20-30 foot high rack storage) from the UL Class III rack-storage tests by using the average B-numbers that were determined experimentally from the bench-scale tests. The heat flux which was convective only resulted in flame heights in best agreement with the experimental data for the bench-scale while the heat flux which gave the best results for the large-scale flame height predictions was the convective

and radiative model for parallel plates. Additional modes of heat flux can be modeled by incorporating correlations for convection and radiation for a specific geometry. Additionally, the heat flux can be further improved on by implementing the flame spread model in a CFD code such as Fire Dynamics Simulator to handle complex geometry, heat flux, and other gas phase issues while the B-number can calculate the resulting mass flux (condensed phase) from various materials.

The B-number can also be directly linked to suppression applications. A critical B-number for extinction can be found experimentally by applying a known amount of water spray to the burning fuel sample until extinction occurs. This could be used in the design of fire sprinkler systems with respect to the location of the sprinklers (spacing and in-rack requirements), the amount of water discharged, and the spray pattern of water from the nozzle. The benefit of using the B-number in this case is that it offers a quantifiable parameter and is linked to the fundamental mass flux principles of the pyrolyzing material.

Finally, the case of mixed commodities and fuels can be further addressed by using the bench-scale method presented here and calculating the B-number for configurations which use various fuel/packaging ratios. Further refinement of the test method can be utilized or perhaps the inclusion of additional nondimensional parameters can capture the mixed fuel interaction that is occurring. Future tests can be instrumented with thermocouples to measure the heat loss between the corrugated cardboard and the polystyrene sample and the heat loss from the back of the polystyrene sample. This can lead to further understanding of the process of energy transfer that occurs when heterogeneous materials are burning as a mixed commodity.

Appendix A - Mass Loss Rates From Bench-Scale Tests

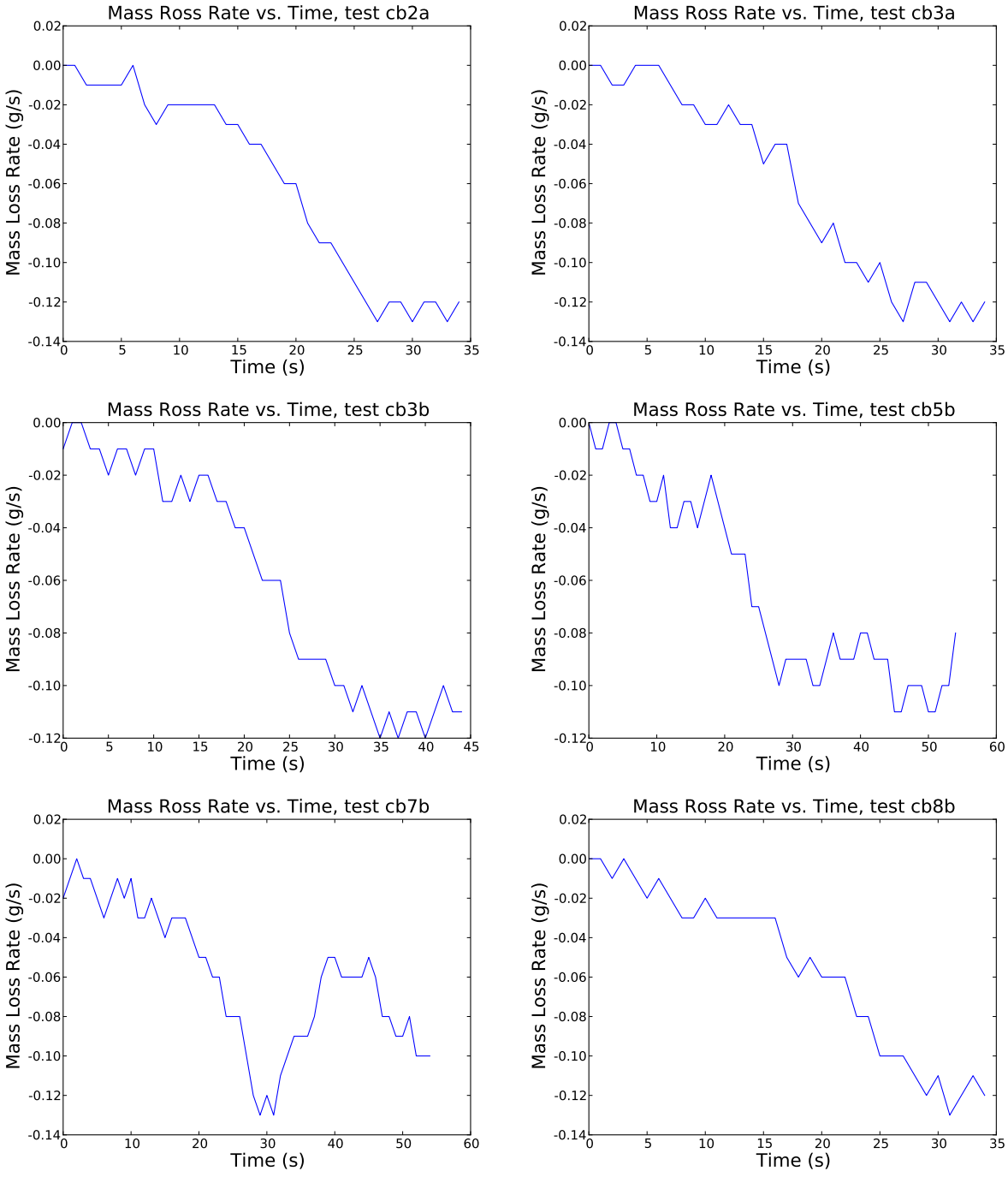

Figure 13: *Mass loss rates vs. time for bench-scale experiments - Corrugated cardboard*

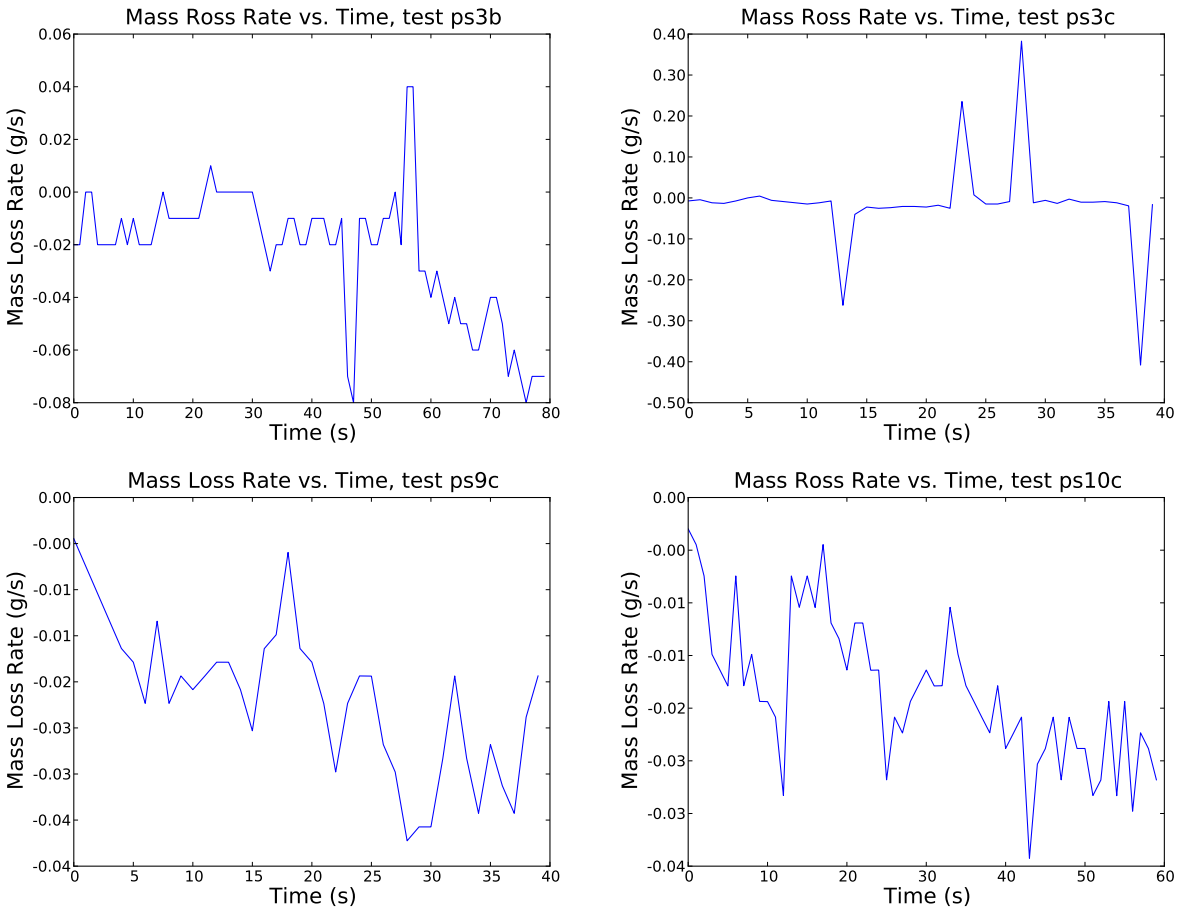

Figure 14: *Mass loss rates vs. time for bench-scale experiments - Polystyrene*

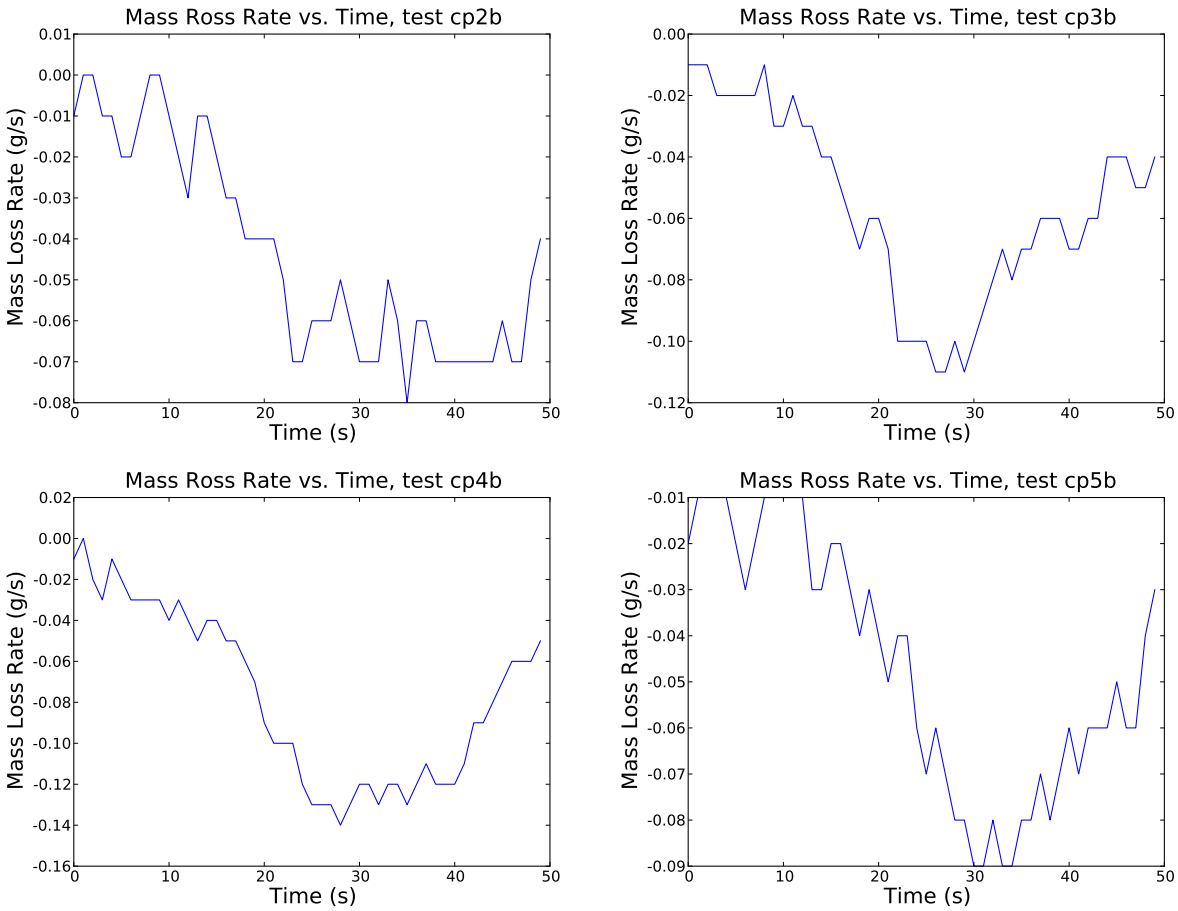

Figure 15: *Mass loss rates vs. time for bench-scale experiments - Corrugated cardboard backed with polystyrene*

Appendix B - B-numbers From Tests

Table 4: Results from B-number calculations

Test name	Material	B-number
cb2a	CB	1.71
cb3a	CB	1.76
cb3b	CB	1.61
cb5b	CB	1.63
cb7b	CB	1.70
cb8b	CB	1.63
ps3b	PS	1.42
ps3c	PS	1.39
ps9c	PS	1.39
ps10c	PS	1.44
cp2b	CB + PS	1.04
cp3b	CB + PS	1.72
cp4b	CB + PS	2.69
cp5b	CB + PS	1.32

Appendix C - Bounding Analysis of B-number for Different Materials

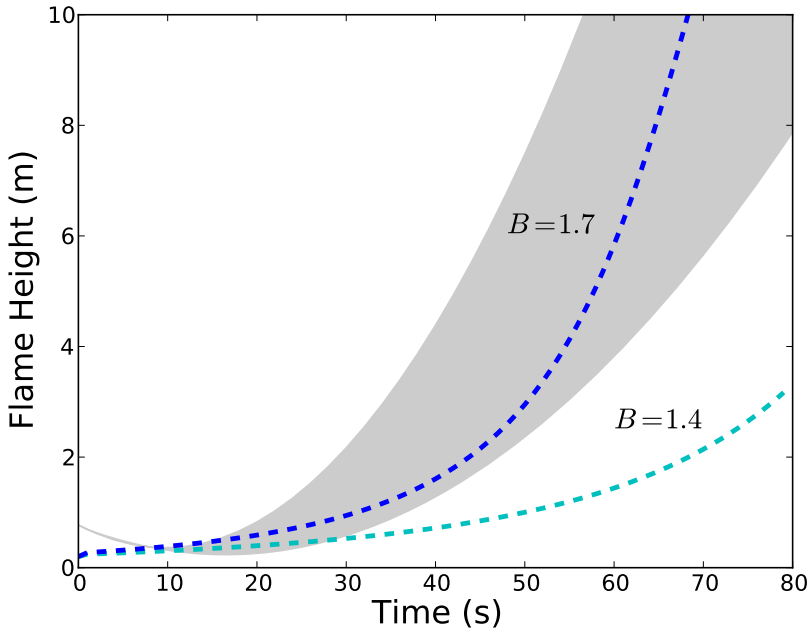

Figure 16: *The dashed lines show large-scale flame height predictions for the B-numbers calculated from the bench-scale tests using corrugated cardboard ($B = 1.7$) and polystyrene ($B = 1.4$). The shaded area represents a range of experimental flame heights from 20-30 foot (6.1 m to 9.1 m) stacks of Class III commodity tests performed at UL for comparison.*

In this study, the flame spread model was validated at the large-scale for corrugated cardboard packed with Class III materials (paper cups), which essentially forms a homogeneous commodity. The flame spread model was shown to perform the best in the case where the mode of heat transfer was most similar to that of the large-scale experimental setup. This mode of heat transfer was represented as the sum of the convective heat transfer plus the radiative heat transfer between parallel plates, which is analogous to the parallel faces of the corrugated cardboard in rack storage. Since the problem has been separated into two processes, heat and mass transfer, it is reasonable that the type of heat transfer modeled in the large scale should best represent the

physical mode of heat transfer in the large-scale, where radiation becomes an important factor in the flame spread process.

The average B-number value obtained from bench-scale tests in this study was 1.7 for corrugated cardboard and 1.4 for polystyrene. Figure 16 shows the range of the large-scale flame height predictions by using the B-number value for both materials and setting all other variables in the flame spread model to remain as fixed values. Heat transfer is modeled the same for both cases by using convective heat transfer plus radiation using the radiant heat transfer correlation for parallel plates as described in Section 5. The soot yield (Y_s) and the thermophysical properties in the flame spread model are set as the properties of corrugated cardboard. Therefore, the flame spread model is not accurately resolving the moving ignition front in the case of the polystyrene flame height predictions but is shown for the purposes of a comparative analysis and sensitivity of the flame spread model to the value of the B-number.

A mixed commodity (such as Group A polystyrene cups contained within corrugated cardboard packaging) tends to behave as a more complex problem where various mixed-fuel interactions are occurring between the different materials. It is hypothesized that this complex problem exists due to the varied heat transfer interaction between the layers of fuels. This was also observed in the small-scale Group A commodity tests performed by Gollner [15]. In these small-scale tests, a single face of a standard commodity box consisted of a corrugated cardboard box packed with Group A plastic (polystyrene) cups, separated by corrugated cardboard dividers. The box tests were ignited on the front face of the corrugated cardboard with all other sides of the box insulated. As the fire grew in size, 3 stages of burning were identified: 1) flame spread along the corrugated cardboard face, 2) inner packing material burned away and the polystyrene heated before ignition, and 3) combustion of polystyrene and remaining corrugated cardboard within the commodity.

In observing the results in the present work, the methodology described attempts to capture the various stages of burning in the mixed commodity tests by calculating the average B-number at the bench-scale. A preliminary approach has been attempted and 4 tests were conducted using samples of corrugated cardboard backed with a polystyrene sheet as described in Section 4. As the corrugated cardboard in the tests burned upwards, some of the heat was being transferred via conduction to the polystyrene material backing. It was observed during the bench-scale, mixed commodity tests that the polystyrene melted and charred to some degree that was inconsistent between the tests. However, none of the mixed commodity tests resulted in successful ignition and sustained burning of the polystyrene sample. More mixed commodity tests can be performed where the heat transfer and interaction between the materials is better measured using thermocouple placement between the fuel samples and behind the backing material to quantify the heat transfer and interaction between the samples.

A framework has been provided towards analyzing this problem of warehouse fire spread. As a preliminary approach, two nondimensional parameters (B and Y_s have been used to show qualitative trends for both the bench-scale and large scale flame heights. However, the results from this study should not be used as a quantitative flammability ranking tool. Various complications exist where further refinement of the test method can be utilized or perhaps the inclusion of additional nondimensional parameters can capture the mixed fuel interaction that is occurring for mixed commodity configurations. More work is needed in the area of mixed fuel interaction. In addition to the mixed fuel interactions, Rangwala et al. [38] found that an experimentally determined B-number changes over time for a material. Fluctuations in the B-number occur both because of time-dependent changes in the material burning, as well as a change in the mixture of constituents burning throughout the box over time. This was observed at both the bench-scale tests performed for this study and in the

small-scale tests performed by Gollner [15].

Appendix D - Thermally-Thin and Thermally-Thick Behavior of Material Samples

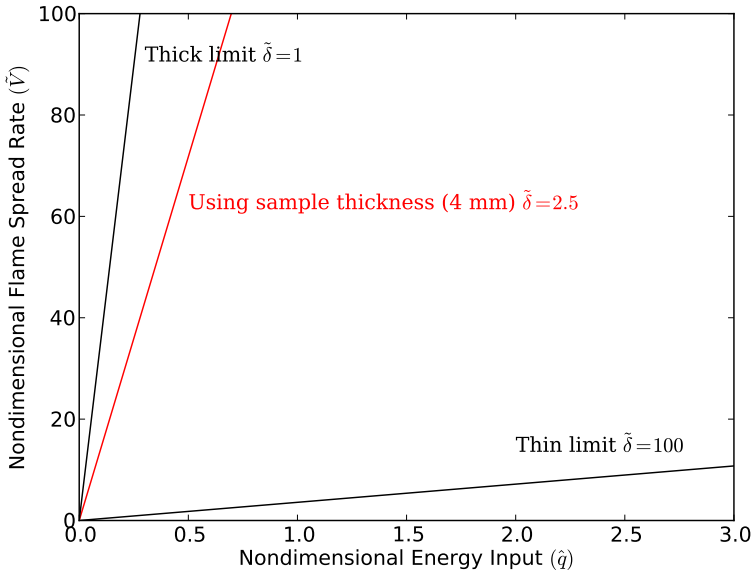

(a) Corrugated cardboard

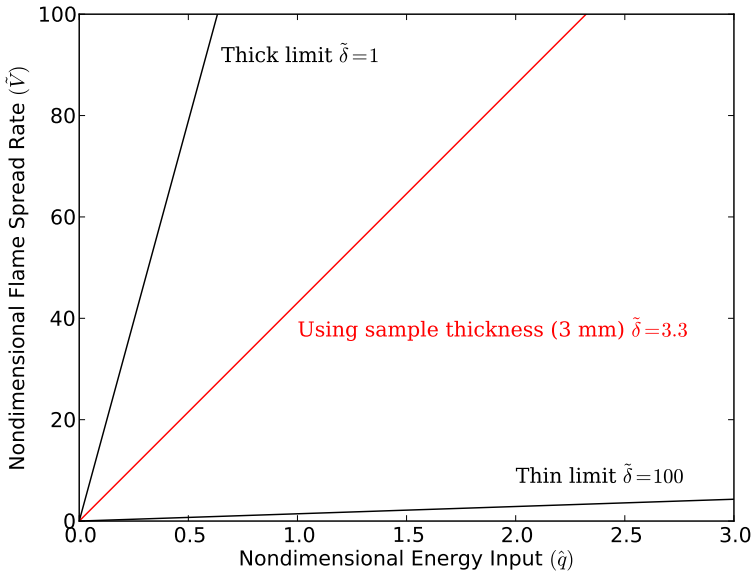

(b) Polystyrene

Figure 17: *The thermal behavior for the two materials used in the bench-scale tests: (a) corrugated cardboard and (b) polystyrene. The thick limit, thermal behavior using the sample thickness, and thin limit are shown for each material.*

The flame spread process was described in Section 5 as a moving ignition front, where the unburned material is heated due to heat flux from the flame above the pyrolysis region. The thickness of the fuel can be an important aspect of flame spread as heat transfer occurs due to conduction from the surface to the interior of the fuel. The rate at which this conduction occurs influences the rate of flame spread. It has been shown theoretically that the rate of flame spread is inversely proportional to the thickness of the material [46]. If a fuel is very thin, it can be treated as a "thermally thin" material, where no temperature gradient exists between the faces of the sample. As the sample thickness increases, the rate of flame spread eventually becomes independent of the sample thickness and the material is said to behave in a "thermally thick" manner.

From the flame spread model that was used in Section 5, the thermal behavior of the samples is examined by varying the value of the sample thickness (τ) and observing at what limits (thin and thick) the rate of flame spread will be independent of the sample thickness. Figure 17 shows the nondimensional flame spread rate $(\tilde{V})$ as a function of the nondimensional energy input $(\hat{q})$ for the corrugated cardboard and polystyrene samples used in the bench-scale tests. The nondimensional flame spread rate $(\tilde{V})$ is given in Equation 7 from Sibulkin and Kim [52] as $\tilde{V} = V\tau/\alpha$ where V is the average flame spread velocity equal to 0.7 cm/s for corrugated cardboard and 0.15 cm/s for polystyrene as determined from the bench-scale tests, τ is the sample thickness, and α is the thermal inertia $(k/\rho_s c_p)$ calculated using the condensed phase properties in Table 3. The nondimensional energy input $(\hat{q})$ is given in Equation 10 from Sibulkin and Kim [52] as $\hat{q} = \dot{q}''(0)\delta/[k(T_p - T_\infty)]$, where $\dot{q}''(0)$ is the surface heat flux at the pyrolysis height, δ is the preheat distance, and k and T_p are the thermal conductivity and the pyrolysis temperature, respectively for the condensed phase.

The nondimensional preheat distance $(\hat{\delta})$ is given by δ/τ, where δ is the preheat distance and τ is the thickness of the sample. Three finite values of $\hat{\delta}$ are shown for each

sample using the condensed phase properties given in Table 3. Each of the three lines shows a variation of the thickness (δ) in $\hat{\delta}$, resulting in (1) the thin limit for the material as $\hat{\delta}$ approaches zero, (2) the thick limit for the material as $\hat{\delta}$ approaches ∞, and (3) the result when τ is set to the thickness of the samples (4 mm for corrugated cardboard and 3 mm for polystyrene) used in the bench-scale tests.

The thermal behavior of the fuel samples used in the tests lies between the thermally thin and thermally thick limits. For upward flame spread, the preheating time is usually very short when compared to lateral or downward flame spread. Therefore, the fuel sample can be considered to behave in a thermally thick manner. The thermal behavior of the corrugated cardboard lies closer to the thick limit since it has a higher flame spread velocity, which results in a shorter time for the material to preheat to its ignition temperature and conduct into the fuel sample.

Appendix E - Pyrolysis Height Fits Used in B-number Calculation

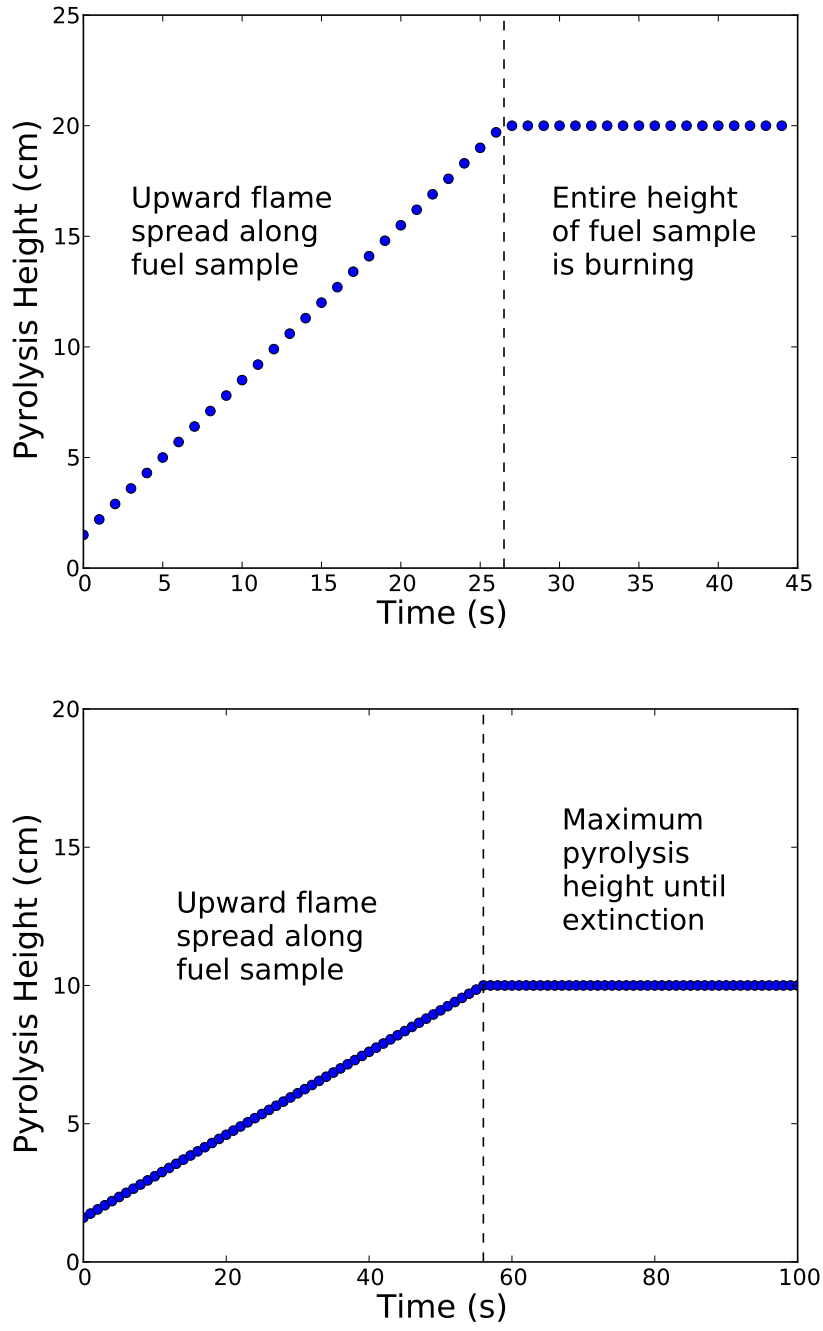

Figure 18: *Pyrolysis height data fits used in average mass-loss rate calculations. The data fits are based on bench-scale tests. Top: Corrugated cardboard; Bottom: Polystyrene*

Appendix F - Poster of "Characterizing the Flammability of Cardboard Using a Cone Calorimeter"

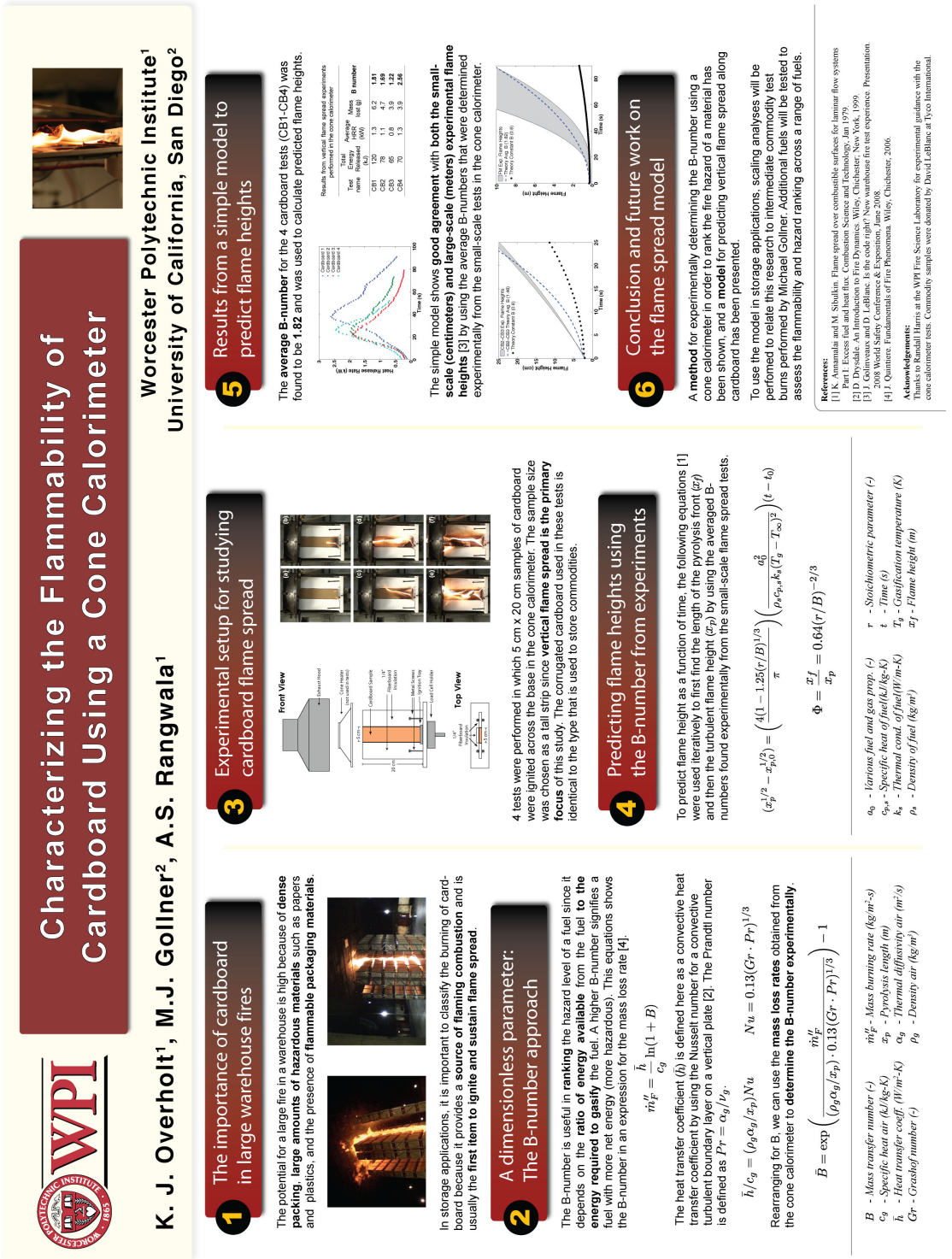

References

[1] L. Nadile. The problem with big. *NFPA Journal*, March/April 2009.

[2] M.J. Gollner. A Fundamental Approach for Storage Commodity Classification. Master's thesis, University of California, San Diego, 2009.

[3] Firehouse.com. "Fire destroys Houston furniture warehouse", July 2009.

[4] T.R. Mariner. "Nine career fire fighters die in rapid fire progression at commercial furniture showroom - South Carolina," Fatality assessment and control evaluation (FACE) investigation report. No. F2007-18, National Institute for Occupational Safety and Health. 2009.

[5] L. Frederick, J.L. Tarley, C. Guglielmo, and T.R. Merinar. "Career fire fighter dies of carbon monoxide poisoning after becoming lost while searching for the seat of a fire in warehouse - New York," Fatality assessment and control evaluation (FACE) investigative report. No. F2004-04, National Institute for Occupational Safety and Health. [5] National Fire Protection Association, "Fire investigation report: supermarket - Phoenix, Arizona (March 14, 2001)," tech. rep., National Fire Protection Association. 2004.

[6] R.F. Duval and S.N. Foley. National Fire Protection Association, "Fire investigation report: supermarket Phoenix, Arizona (March 14, 2001)," tech. rep., 2001.

[7] F. Washenitz, K. Cortez, T. Mezzanotte, M. McFall, T. Merinar, T. McDowell, and V. Dunn. "Warehouse fire claims the life of a battalion chief - Missouri," fatality assessment and control evaluation (FACE) investigative report. No. 99-F48, National Institute for Occupational Safety and Health. 1999.

[8] R.W. Braddee, T.R. Merinar, T.P. Mezzanotte, T. Pettit, N.T. Romano, and F.C. Washenitz. "Six career fire fighters killed in cold-storage and warehouse building fire - massachusetts," Fatality assessment and control evaluation (FACE) investigative report. No. 99-F47, National Institute for Occupational Safety and Health. 2000.

[9] NFPA. "NFPA fire investigations report, bulk retail store fire, Albany, GA, April 16, 1996," tech. rep., National Fire Protection Association, Quincy, MA., 1997.

[10] R.G. Zalosh. *Industrial fire protection engineering*. John Wiley and Sons, 2003.

[11] R.K. Dean. A final report on fire tests involving stored plastics. *Fire Technology*, 12(1):55–65, 1976.

[12] Factory Mutual Insurance Company. FM Global Property Loss Prevention Data Sheet 8-1. 2004.

[13] M.J. Gollner, T. Hetrick, A.S. Rangwala, J. Perricone, and F.A. Williams. Controlling parameters involved in the burning of standard storage commodities: A fundamental approach towards fire hazard classification. Ann Arbor, MI, University of Michigan, May 2009. 6th U.S. National Combustion Meeting.

[14] *NFPA 13: Standard for the Installation of Sprinkler Systems*. National Fire Protection Association, 2007.

[15] M.J. Gollner, K.J. Overholt, F.A. Williams, A.S. Rangwala, and J. Perricone. Warehouse Commodity Classification from Fundamental Principles. Part I: Commodity & Burning Rates. *Fire Safety Journal, In Review*, 2010.

[16] JL Harrington. Lessons learned from understanding warehouse fires. *Fire Protection Engineering, Winter, 2006*.

[17] G. Grant and D. Drysdale. Numerical modelling of early flame spread in warehouse fires. *Fire Safety Journal*, 24(3):247–278, 1995.

[18] A. Hamins and K.B. McGrattan. Reduced-scale experiments on the water suppression of a rack-storage commodity fire for calibration of a CFD fire model. *NIST Technical Report NISTIR*, 6439:457–468, 1999.

[19] K. Saito, J.G. Quintiere, and F.A. Williams. Upward turbulent flame spread. *Fire Safety Science—Proceedings of the First International Symposium*, pages 75—86, Oct 1985.

[20] B. Karlsson. A mathematical model for calculating heat release rate in the room corner test. *Fire Safety Journal*, 20:93–113, 1993.

[21] N. Alvares, H.K. Hasegawa, K. Hout, A.C. Fernandez-Pello, and J. White. Analysis of a run-away high rack storage fire. *Fire Safety Science – Proceedings of the Fourth International Symposium*, pages 1–12, Aug 1994.

[22] H. Ingason and J. de Ris. Flame heat transfer in storage geometries. *Fire safety journal*, 31(1):39–60, 1998.

[23] H. Ingason. Plume flow in high rack storages. *Fire Safety Journal*, 36(5):437–457, 2001.

[24] J. de Ris and L. Orloff. Flame heat transfer between parallel panels. *IAFSS*, 7:1–12, Nov 2003.

[25] J. de Ris, G.H. Markstein, L. Orloff, and P. Beaulieu. Similarity of turbulent wall fires. *Fire Safety Science - Proceedings of the Seventh International Symposium*, 7:259–269, Nov 2003.

[26] Marianne Foley. *The Use of Small Scale Fire Test Data for the Hazard Assessment of Bulk Materials*. PhD thesis, University of Edinburgh, 1995.

[27] M. Foley and D. Drysdale. Heat transfer from flames between vertical parallel walls. *Fire Safety Journal*, 24:53–73, 1995.

[28] F.P. Incropera and D.P. DeWitt. *Introduction to Heat Transfer*. Wiley, New York, 2007.

[29] G.H. Markstein and J. de Ris. Radiant emission and absorption by laminar ethylene and propylene diffusion flames. *Proc. Comb. Inst. 20*, pages 1637–1646, 1985.

[30] D.B. Spalding. Combustion of a single droplet and of a fuel spray. *Selected combustion problems: fundamentals and aeronautical applications*, page 340, 1954.

[31] H.W. Emmons. The film combustion of liquid fuel. *Z. Angew. Math. Mech.*, pages 60–71, 1956.

[32] F.J. Kosdon, F.A. Williams, and C. Buman. Combustion of vertical cellulosic cylinders in air. *Proc. Comb. Inst. 12 (1969)*, pages 253–264.

[33] J.S. Kim and J. de Ris. Laminar burning between parallel fuel surfaces. *International Journal of Heat and Mass Transfer*, 17:439–451, Jan 1974.

[34] R.S. Silver. Application of the Reynolds Analogy to Combustion of Solid Fuels. *Nature,*, London 165:75, 1950.

[35] TH Chilton and AP Colburn. Mass transfer (absorption) coefficients prediction data-on heat transfer fluid motion, Ind. *Industr. Engng Chem*, 26:1183–1187, 1934.

[36] V. Raghavan, A.S. Rangwala, and J.L. Torero. Laminar flame propagation on a horizontal fuel surface: Verification of classical Emmons solution. *Combustion Theory and Modelling*, 13(1):121–141, 2009.

[37] D.B. Spalding. Experiments on the burning and extinction of liquid fuel spheres. *Fuel*, 32:169–185, 1953.

[38] A.S. Rangwala, S.G. Buckley, and J.L. Torero. Analysis of the constant B-number assumption while modeling flame spread. *Combustion and Flame*, 152(3):401–414, Feb 2008.

[39] D.J. Holve and R.F. Sawyer. Diffusion controlled combustion of polymers. *Proc. Comb. Inst. 15 (1975)*, pages 351–361.

[40] K. Annamalai and M. Sibulkin. Flame spread over combustible surfaces for laminar flow systems Part II: Flame heights and fire. *Combustion Science and Technology*, 19(5):185–193, 1979.

[41] K. Annamalai and M. Sibulkin. Flame spread over combustible surfaces for laminar flow systems Part I: Excess fuel and heat flux. *Combustion Science and Technology*, 19(5):167–183, 1979.

[42] A.S. Rangwala. Flame Spread Analysis using a Variable B-Number. *Proc. Fire Safety Sci.*, 9, 2008.

[43] F.A. Williams. *Theoretical studies in heterogeneous combustion*. PhD thesis, California Institute of Technology, 1951.

[44] Y. Pizzo, J.L. Consalvi, P. Querre, M. Coutin, L. Audouin, B. Porterie, and J. L. Torero. Experimental observations on the steady-state burning rate of a vertically oriented PMMA slab. *Combustion and Flame*, 152(3):451–460, 2008.

[45] L. Orloff, J. de Ris, and G.H. Markstein. Upward turbulent fire spread and burning of fuel surface. *Fire and Explosion Research*, pages 1–10, Aug 1974.

[46] D. Drysdale. *An Introduction to Fire Dynamics*. Wiley, Chichester; New York, 1999.

[47] Kristopher Overholt. Characterizing the Flammability of Storage Commodities Using an Experimentally Determined B-number. Master's thesis, Worcester Polytechnic Institute, 2009.

[48] J.G. Quintiere. *Fundamentals of Fire Phenomena*. John Wiley, Chichester, 2006.

[49] C.K. Law and F.A. Williams. Kinetics and convection in the combustion of alkane droplets. *Combustion and Flame*, 19:393–405, 1972.

[50] Stephen R Turns. *An Introduction to Combustion: Concepts and Applications*. McGraw-Hill, New York, 2000.

[51] P.J. Pagni and T.M. Shih. Excess Pyrolyzate. *Proc. Comb. Inst. 16*, pages 1329–1343, 1977.

[52] M. Sibulkin and J. Kim. The Dependence of Flame Propagation on Surface Heat Transfer II: Upward Burning. *Combustion Science and Technology*, pages 1–11, Sep 1977.

[53] R.E. Mark. *Handbook of Physical and Mechanical Testing of Paper and Paperboard*, volume 2. Marcel Dekker, Inc. New York and Basel, 1984.

[54] *SFPE Handbook of Fire Protection Engineering*. National Fire Protection Association; Society of Fire Protection Engineers, Quincy, MA.; Bethesda, MD, 2002.

[55] Y. Xin and M.M. Khan. Flammability of combustible materials in reduced oxygen environment. *Fire Safety Journal*, 42(8):536–547, 2007.

[56] J. Golinveaux and D. LeBlanc. Is the code right? New warehouse fire test experience. Presentation. 2008 World Safety Conference & Exposition. Las Vegas, NV, June 2008.